ACIDIZING DOLOMITE RESERVOIRS USING HCL ACID PREPARED WITH SEAWATER: PROBLEMS AND SOLUTIONS

A Thesis

by

DENNIS GEORGE ARENSMAN

Submitted to the Office of Graduate and Professional Studies of
Texas A&M University
in partial fulfillment of the requirements for the degree of

MASTER OF SCIENCE

Chair of Committee,	Hisham A. Nasr-El-Din
Committee Members,	Robert Lane
	Mahmoud El-Halwagi
Head of Department,	A. D. Hill

May 2014

Major Subject: Petroleum Engineering

ABSTRACT

Seawater is the only viable water source for many offshore wells with dolomite formations. For these wells it is important to use compatible fluids when stimulating to avoid damaging the formation with calcium sulfate precipitation. Much work has been conducted on this problem for limestone, but there have been no publications about calcium sulfate precipitation within dolomite during matrix acidizing. This work quantifies permeability damage when acidizing using hydrochloric acid mixed with seawater and no scale inhibitors. Scale inhibitors were also tested for effectiveness in reducing calcium sulfate scale during acidizing.

Static jar tests of three phosphonate-based, two sulphonated polymer-based, and one polyacrylic-based scale inhibitors in spent acid systems were used to compare the effectiveness at temperatures ranging from 77 to 325°F. Corefloods were conducted to investigate the extent of calcium sulfate precipitation without scale inhibitors and to test permeability improvements with the addition of compatible scale inhibitors at temperatures up to 325°F.

This work shows that calcium sulfate precipitation within dolomite during matrix acidizing with seawater and hydrochloric acid will damage the well. Corefloods with seawater showed a permeability reduction of 30% or greater compared to corefloods with freshwater for all temperatures tested when no scale inhibitors were included in the acid solution. Calcium sulfate precipitation was determined to be the cause of the decreased permeability. DTPMP, a phosphonate-based scale inhibitor, and a sulfonated

polymer scale inhibitor at concentrations of 150 ppm were shown to effectively reduce calcium sulfate scale with minimal inhibitor/rock reaction during these tests. The ability to improve stimulation effectiveness by the addition of compatible scale inhibitors to the acid solution is critical information to prevent damaging dolomite formations during matrix acidizing with hydrochloric acid and seawater.

DEDICATION

This work is dedicated to my parents and my fiancée, Holly.

ACKNOWLEDGEMENTS

I would like to thank my committee chair, Dr. Nasr-El-Din, and my committee members, Dr. Lane, and Dr. El-Halwagi, for their guidance and support throughout this research.

Thanks also go to my friends and colleagues and the department faculty and staff for making my time at Texas A&M University a great experience. I also want to extend my gratitude to the Acid Stimulation Research Project funding for this research.

Finally, I give thanks to my mother and father for their encouragement and to my fiancée for her patience and love.

NOMENCLATURE

DI Water	Deionized water
HCl	Hydrochloric Acid
k	Permeability
k_f	Final Permeability
k_i	Initial Permeability
mD	Millidarcy
P	Pressure
SI	Scale Inhibitor
SW	Seawater
T	Temperature
t	Time
TDS	Total Dissolved Solids
ϕ	Porosity

TABLE OF CONTENTS

Page

LIST OF FIGURES

Page

LIST OF TABLES

Page

1. INTRODUCTION

1.1 Background

Stimulating carbonate reservoirs by injecting HCl into the reservoir is a common technique that has been used in the field for decades. Both calcite and dolomite reactions with HCl have been well studied[1]. In a perfect open system at standard temperature and pressure with pure dolomite and HCl reaction the reaction is as follows:

$$CaMg(CO_3)_2 + 4HCl \rightarrow CaCl_2 + MgCl_2 + 2CO_2\uparrow + 2H_2O \quad (1\text{-}1)$$

During the reaction calcium and magnesium ions are released into solution to bond with monovalent and divalent ions; which leads to the potential for scales to form.

Local water sources are the main source of water injected into oilfields. In offshore locations the only local source of water is seawater. During stimulation treatments, seawater can be used during every stage of the operation from pre-flush to post-flush including diluting acids. Seawater contains high concentrations of sulfate, which can lead to the following reactions during matrix acidizing of dolomite;

$$Ca^{2+} + SO_4^{2-} + xH_2O \rightarrow CaSO_4 \cdot xH_2O\downarrow \quad (1\text{-}2)$$

where x=0, 1/2, and 2 and,

$$Mg^{2+} + SO_4^{2-} + xH_2O \rightarrow MgSO_4 \cdot xH_2O. \quad (1\text{-}3)$$

Magnesium sulfate is soluble in all conditions present within the oilfield so the reaction shown in (1-3) does not need to be considered, but calcium sulfate will precipitate in field conditions. The forms of calcium sulfate that can occur are anhydrite ($CaSO_4$), hemihydrate ($CaSO_4 \cdot 1/2H_2O$), and gypsum ($CaSO_4 \cdot 2H_2O$). Gypsum is the stable phase

up to 40°C, anhydrite is the stable phase above 120°C, and hemihydrate is the stable phase at intermediate temperatures with high TDS brines[2]. Temperature and ionic strength are the predominant factors affecting calcium sulfate solubility with other factors, like pH and flow rate, having a smaller influence on the scale solubility[3].

Scale inhibitors are included during matrix acidizing treatments to prevent scales from forming and have two main inhibition mechanisms: nucleation inhibition and crystal growth inhibition[4]. Nucleation inhibition is the prevention of scales from starting to form crystals while crystal growth inhibition is the prevention of already formed scale crystals from growing. Scale inhibitors have been tested in acidic calcite environments, for squeeze treatments, and for water injection in all types of carbonate environments for various types of scales[5]. Unfortunately every environment is different and testing of various scale inhibitors is always required to find the best scale inhibitor for each environment.

1.2 Previous Work

Previous work similar to the experiments discussed later have been conducted on the reduction of calcium sulfate scale during matrix acidizing of carbonates[5c, 5d, 6], but the authors tested calcite and not dolomite while claiming the result held true for all carbonates. The problem with assuming results from work with calcite is true for all carbonates is that calcium sulfate is dependent on ion concentration within the brine for solubility and crystal structure[2b] and scale inhibitors are dependent on both ion concentration within the brine and the Ca^{2+}/Mg^{2+} ratio[7]. Differences in rock mineralogy

cause calcite that is acidized with HCl to release twice as many calcium ions as dolomite. Also, dolomite contains magnesium ions which are not present in calcite. For these reasons dolomite needs to be analyzed separately from calcite for scaling tendencies and scale inhibitor compatibility.

1.3 Statement of Problem

Seawater is the only viable source of surface water for injection in an increasing number of wells. If the seawater is compatible with the formation brine, then this practice will not cause additional damage to the well. However, when hydrochloric acid is injected into a dolomite reservoir with seawater present, the calcium ions released during the dolomite dissolution will bond with free sulfate ions within seawater to form calcium sulfate scale. The flow path within the dissolved dolomite is then restricted by calcium sulfate scale attaching to pore walls and pore throats. Scale inhibitors can be added in order to mitigate scale formation, but not all scale inhibitors will effectively prevent calcium sulfate scale. Furthermore, not all scale inhibitors are compatible with the high salinity environment, which may result in precipitation.

1.4 Objectives

Experiments were designed to quantify damage caused by acidizing dolomite with HCl in the presence of seawater. The potential of various scale inhibitors to inhibit scale formation under conditions that promote scale formation during acidizing of dolomite with HCl was examined and quantified using the permeability change resulting

from the treatment. Finally, the results from these experiments will be compared with results from studies on calcite.

2. EXPERIMENTAL METHODS

2.1 Acid Preparation

ACS grade HCl was diluted to 15 wt% using either DI water or seawater. The diluting fluid was matched with the pre- and post- flush fluids for each experiment.

2.2 Seawater Preparation

Table 1 below shows the average seawater composition from locations around the world and the composition of seawater at the Arabian Gulf at Kuwait. The composition of seawater for the Arabian Gulf at Kuwait has a very high sulfate concentration for seawater. For these studies high sulfate concentration was desired, so synthetic seawater was created according to the composition of seawater at Arabian Gulf at Kuwait. The table lists the salt concentration in ppm. To create the synthetic seawater, first the salts were weighed out and added to the desired volume of water. Then, the salts and water were mixed with an overhead mixer at 450 rpm until no visible salts remained in the water.

Table 1: Table of ion concentrations in seawater at different locations around the world and the average ion concentration within seawater. Concentrations in the table are shown in units of ppm.

	Typical Seawater	Arabian Gulf at Kuwait
Chloride (Cl^-)	18,980	23,000
Sodium (Na^+)	10,556	15,850
Sulfate (SO_4^{2-})	2,649	3,200
Magnesium (Mg^{2+})	1,262	1,765
Calcium (Ca^{2+})	400	500
Potassium (K^+)	380	460
Bicarbonate (HCO_3^-)	140	142
Strontium (Sr^{2+})	13	-
Bromide (Br^-)	65	80
Borate (BO_3^{3-})	26	-
Fluoride (F^-)	1	-
Silicate (SiO_3^{2-})	1	1.5
Iodide (I^-)	<1	-
Others	-	-
Total Dissolved Solids (TDS)	34,483	45,000

2.3 Core Preparation

Dolomite cores were first cut into cylinders of 1.5 inch diameter by 6 inch length. The cut cores were then placed in a 250°F oven for 4 hours to dehydrate the cores. Each core was then weighed to get the dry weight of the core. Next, the cores were saturated in either DI water or seawater. The initial permeability for each core was then measured

using the coreflood at a minimum two different flow rates; preferably three flow rates were used. Cores with initial permeability in the range 0.3 to 4 mD were tested in these experiments. If the core was later decided to be used for seawater application these steps would be repeated and seawater would be substituted for DI water. Each core was reweighed after the saturation step to obtain the saturated weight. Each core's porosity was calculated from the wet and dry weight of each core.

2.4 Corefloods

Figure 1 shows the piping and instrument diagram of the coreflood set-up used in these studies. Pressure is applied to each fluid cylinder by the syringe pump at a constant flow rate. Each valve above the pistons can be opened and closed independently to select which fluid is pushed through the coreflood. An effluent sample collection area is set-up to collect fluid exiting the core holder in test tubes or a waste container. Pressure drop across the core is measured using a pressure gauge with lines connected to each end of the core holder, and then recorded electronically as the pressure gauge transmits the recorded values to a computer.

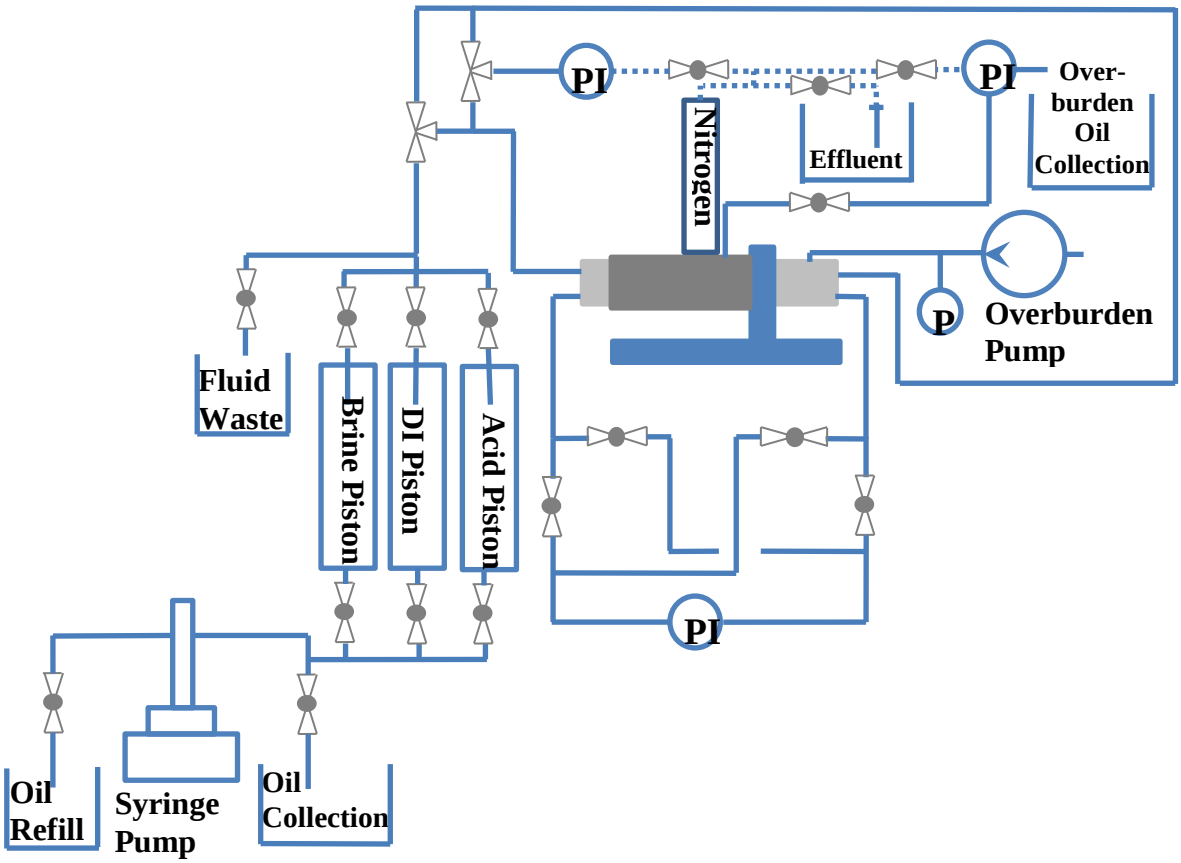

Figure 1: Piping and instrument diagram of coreflood set-up.

Figure 2 shows a cross-sectional view of the core holder used in these studies. Within the metal frame is an overburden sleeve surrounded by oil. A core is placed within the overburden sleeve so that when pressure is applied to the overburden sleeve flow around the core is restricted. Oil around the overburden sleeve can be added to increase pressure applied by using a hand pump.

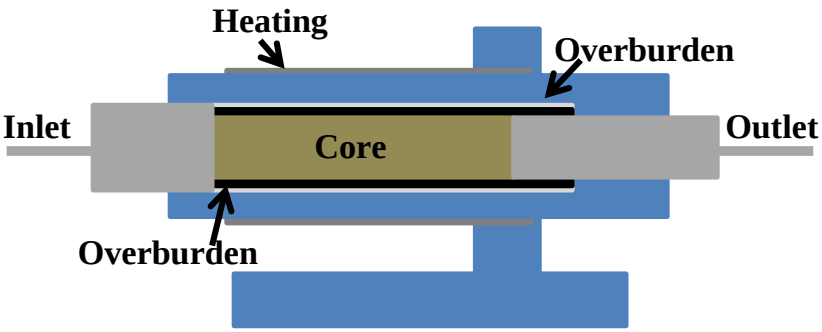

Figure 2: Cross-section view of core holder.

Corefloods testing initial permeability used an overburden pressure of 2000 PSI, a back pressure of 0 PSI, and a temperature of 77°F. Corefloods during the acidizing experiments used an overburden pressure of 2000 PSI, a back pressure of at least 1000 PSI, and a temperature of 77°F, 150°F, 250°F, or 325°F, depending on the experiment. Backpressure was maintained above 1000 psi during acidizing tests to prevent the release of CO_2 generated by the reactions within the core. After the core was placed in the core holder the saturation fluid would be injected through the core until equilibrium conditions within the core were achieved. Then, the temperature would be raised to the desired level (if applicable) and the conditions would be allowed to return to equilibrium. After equilibrium conditions were achieved, 20 mL of acid would be injected through the core followed by a post-flush of the original saturation fluid. The experiment would conclude once equilibrium conditions, based on sulfate concentration of collected samples, were observed once again.

2.5 Static Jar Tests

Solutions were mixed to simulate the spent acid environment with dolomite according to Table 2. For these tests, the salts were mixed with 40 mL of synthetic seawater and 1 wt% HCl. Scale inhibitors were added to the synthetic spent acid environment according to Table 3. Then, the sample was placed within a Hassler-type visual cell, shown in Figure 3, and brought to the desired temperature. Samples were exposed to test temperatures for 30 minutes to allow the full amount of scale to precipitate. According to He et al. (2013) scale inhibitors will be least effective during the 1 wt% partially spent HCl condition during matrix acidizing.

Table 2: Weight of salts added to 40 mL of synthetic seawater to create a synthetic environment of (partially) spent acid in dolomite.

Salts Added to Simulate 40 mL (Partially) Spent Acid Environment in Dolomite					
	15 wt% HCl	10 wt% Partially Spent HCl	5 wt% Partially Spent HCl	1 wt% Partially Spent HCl	Completely Spent HCl
Density, g/cm^3	1.07	1.11	1.16	1.18	1.19
Volume, cm^3	10	10	10	10	10
$MgCl_2 \cdot 6(H_2O)$, g Added to Mixture	0	1.479	3.062	4.442	4.795
$CaCl_2 \cdot 2(H_2O)$, g Added to Mixture	0	1.167	2.417	3.506	3.784

Table 3: Volume of scale inhibitor added to 40 mL 1 wt% partially spent acid sample to obtain a desired inhibitor concentration.

Volume of Scale Inhibitors Added to 40 mL Partially Spent Acid Environment								
Scale inhibitor Concentration, mg/L		50	100	150	250	500	1000	10000
	Density, g/ml	**Volume Scale Inhibitor (µL) for a 40 mL Sample**						
PPCA, ml	1.11	1.80	3.60	5.41	9.01	18.02	36.04	360.4
Sulfonated Polymer, ml	1.22	1.64	3.28	4.92	8.20	16.39	32.79	327.9
PAA, ml	0.9791	2.04	4.09	6.13	10.21	20.43	40.85	408.5
P-tagged Sulfonated Polymer, ml	1.34	1.49	2.99	4.48	7.46	14.93	29.85	298.5
DTPMP, ml	1.1	1.82	3.64	5.45	9.09	18.18	36.36	363.6
BHMT, ml	1.075	1.86	3.72	5.58	9.30	18.60	37.21	372.4
							Sample Size	
							40.00 mL	

A 1 wt% partially spent acid solution was prepared using seawater. Then, the scale inhibitor was added, and finally $CaCl_2$ and $MgCl_2$ were added according to calculations in Table 2.

Figure 3: VCL Series visual cell.

3. DAMAGE CAUSED BY ACIDIZING DOLOMITE IN THE PRESENCE OF SEAWATER

3.1 Introduction

Acid reaction with calcite is much faster than acid reaction with dolomite. Reaction rates of HCl and dolomite will increase as temperature increases until the reaction is transport limited rather than reaction rate limited at about 200°F [8]. Clays such as illite within the dolomite, however, can slow or even prevent the rock from reacting with the HCl because they do not react with HCl and will form an impenetrable layer for the acid when the surrounding rock is dissolved [1c].

When acid is injected into a core too slowly a single wormhole with a large diameter will form, at too high of flow rates many small wormholes will form [9]. This is caused by the reaction rate of acid and the flow rate of the acid resulting in 1) high reaction rates and low flow rates that allow the acid to form a dominant channel with higher permeability which will encourage more acid to flow through that same wormhole and continuously increase the size of the dominant wormhole, or 2) low reaction rates and high flow rates that allow the acid to form many small wormholes since the acid will not have time to dissolve a single wormhole to encourage acid to continue flowing along the same path. In laboratory corefloods if the reaction rate is very high and the flow rate is very low, a phenomenon called face dissolution occurs on the core, which is when the acid reacts completely with the core before it enters the core. This causes the inlet of the core to be dissolved and no wormholes to form. For the

current set of experiments, face dissolution needs to be avoided to allow over-saturation conditions to occur within the core; not before entering the core. Formation of the other two types of wormholes is desirable since both will allow over-saturation conditions to be created within the core.

Magnesium that is freed during the dissolution of dolomite by HCl will bond with the free sulfates when seawater is present in quantities allowing over-saturation conditions to exist. Magnesium sulfate has many crystal forms with water, such as $MgSO_4$, $MgSO_4 \cdot H_2O$, $MgSO_4 \cdot 2H_2O$, $MgSO_4 \cdot 7H_2O$, et cetera, and all of these forms are soluble in water at all reservoir conditions [10]. This means that magnesium sulfate is not a potential source of damage during the coreflood experiments.

Calcium that is freed during the dissolution of dolomite by HCl will bond with the free sulfates when seawater is present in quantities allowing over-saturation conditions to exist. Calcium sulfate has three different forms: anhydrite ($CaSO_4$), hemihydrate ($CaSO_4 \cdot 1/2H_2O$), and gypsum ($CaSO_4 \cdot 2H_2O$) [11]. Below 40°C gypsum is the predominant stable form of calcium sulfate scale that will form and above 120°C anhydrite is the predominant form of calcium sulfate scale that will form. The Solubility of Gypsum decreases with increased temperature above 40°C while the solubility of hemihydrate and anhydrite decreases with increases temperature at all temperatures. Pressure does not affect the solubility of any form of calcium sulfate. Calcium sulfate will start to grow gypsum crystals at pH values as low as 4.5 to 6.6 and at lower pH values 2.3 hemihydrate and gypsum crystals that form will slowly transform into anhydrite [12].

Precipitated crystals will form along walls and pore throats. Any scale that forms along pore throats restricts flow 3-4 times more than scale that forms along walls [13]. So long as the scale precipitates while in the bulk solution, the Peclet number will describe the deposition of particles in the absence of particle/pore repulsions. Veerapen also found that scale deposition diminished as flow rate increased.

3.2 Results

In order to determine the amount of damage caused by sulfate precipitation, corefloods were run using DI water and seawater at predetermined temperatures. The temperatures tested were 77, 150, 250, and 325°F. Side-by-side comparison shows how much the dolomite would be stimulated in an ideal case (no sulfate present) and how much stimulation, or damage, there is in the non-ideal case (sulfate present). The comparison creates a quantifiable amount of damage caused by calcium sulfate precipitation within this system by comparing the ratio of final permeability to initial permeability (k_f/k_i) from each case.

3.2.1 Temperature = 77°F

The DI water coreflood at 77°F increased the permeability within the core while not causing breakthrough. The k_f/k_i ratio for this case was 1.14 meaning stimulation occurred. Figure 4 shows the graph of the pressure drop across the core for this experiment and it shows how the pressure drop across the core corresponds to the introduction of each fluid. Figure 5 shows the graph of pressure drop across the core

compared with the concentration of dissolved calcium and magnesium in the collected effluent samples. The rise and fall of the calcium and magnesium concentrations correspond with the introduction and removal of acid from the system. The calcium concentrations reached below supersaturation concentrations by the end of the experiment indicating that no precipitation of calcium carbonate could take place after the coreflood. Sulfate was not measured during this experiment, nor during any other experiment with DI water as the pre- and post- flush fluid, because no sulfate was introduced into the core during the coreflood. Figure 6 shows a comparison between the pressure drop across the core and the pH of the collected effluent samples. The pH lowers when HCl is added to the system as expected, and then rises after DI Water is re-injected through the core.

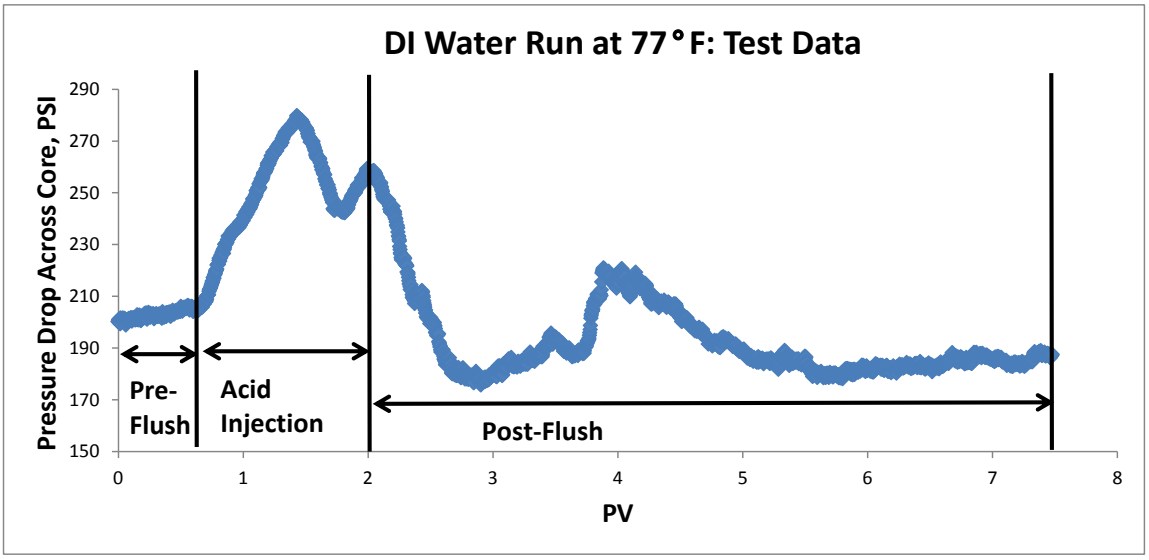

Figure 4: Graph of pressure drop across the tested core for the 77°F DI Water experiment.

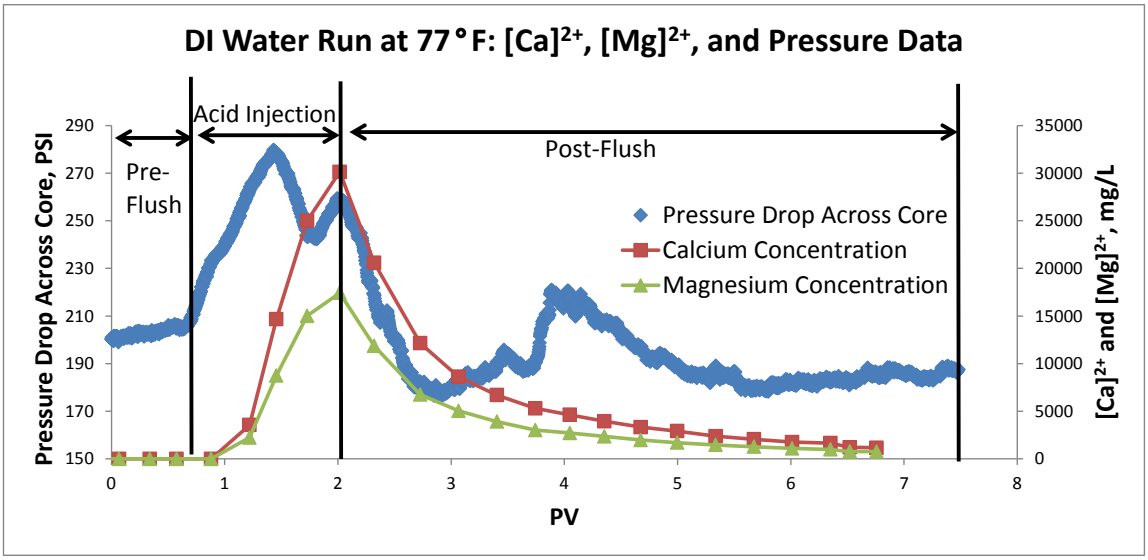

Figure 5: Graph of pressure drop across the tested core compared to dissolved calcium and magnesium concentrations within collected effluent samples for the 77°F DI Water experiment.

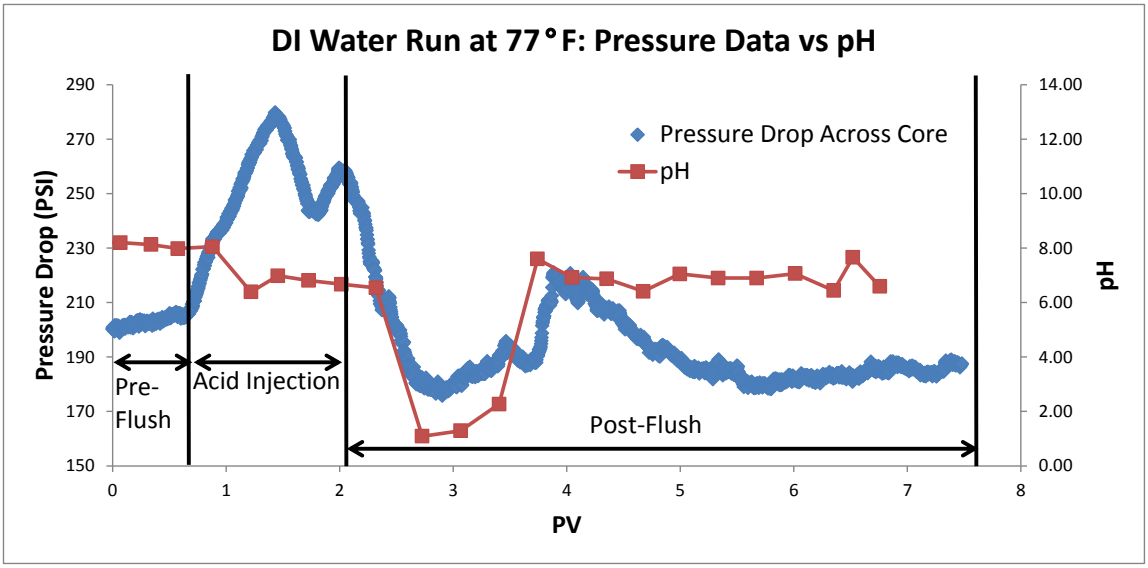

Figure 6: Graph of pressure drop across the tested core compared to the pH of the collected effluent samples for the 77°F DI Water experiment.

The coreflood using seawater and no scale inhibitors at 77°F showed large amounts of damage caused by sulfate scale formation. This core was damaged as shown

by the k_f/k_i ratio of 0.93. Figure 7 shows the graph of pressure drop across the core for this experiment and Figure 8 shows the graph comparing calcium and magnesium ratios in collected samples to the pressure drop across the core. Both of these graphs have similar trends to the ones for the experiment with DI Water at 77°F. Figure 9 shows the comparison of pH in the collected effluent samples to pressure drop across the core. There was less of a drop in pH in the collected samples this time indicating that the acid reacted more fully in this test than in the DI water test. Sulfate concentration was measured immediately after the coreflood and after a delay of at least 24 hours which allowed all scaling products to fully react and bring the chemicals within the sample to saturation levels as shown in Figure 10.

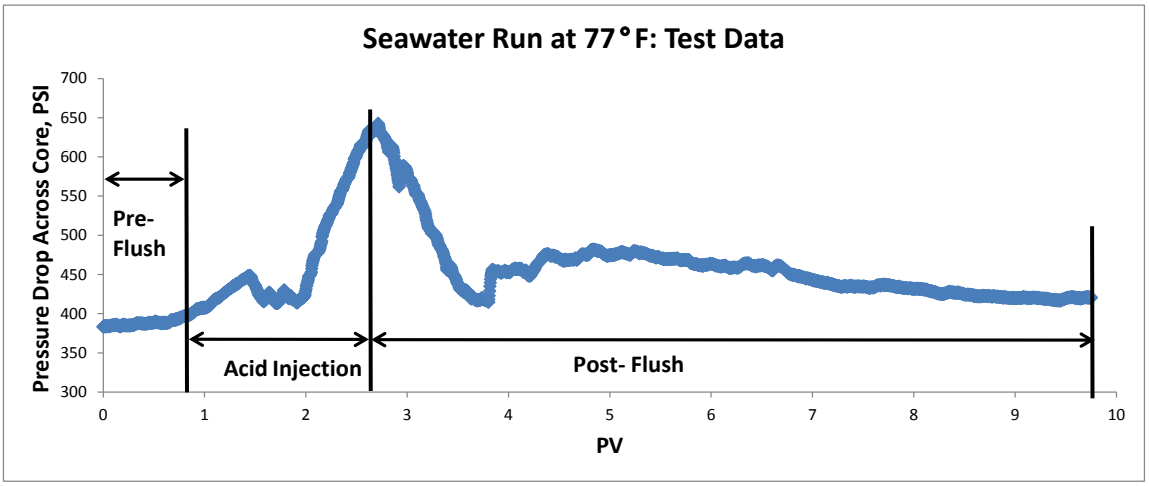

Figure 7: Graph of pressure drop across the tested core for the 77°F seawater experiment.

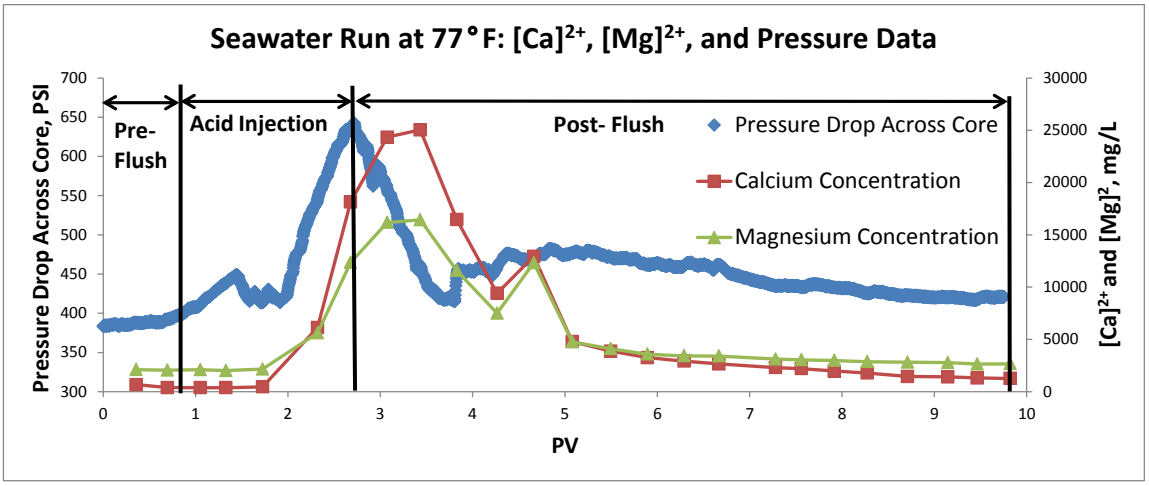

Figure 8: Graph of pressure drop across the tested core compared to dissolved calcium and magnesium concentrations within collected effluent samples for the 77°F seawater experiment.

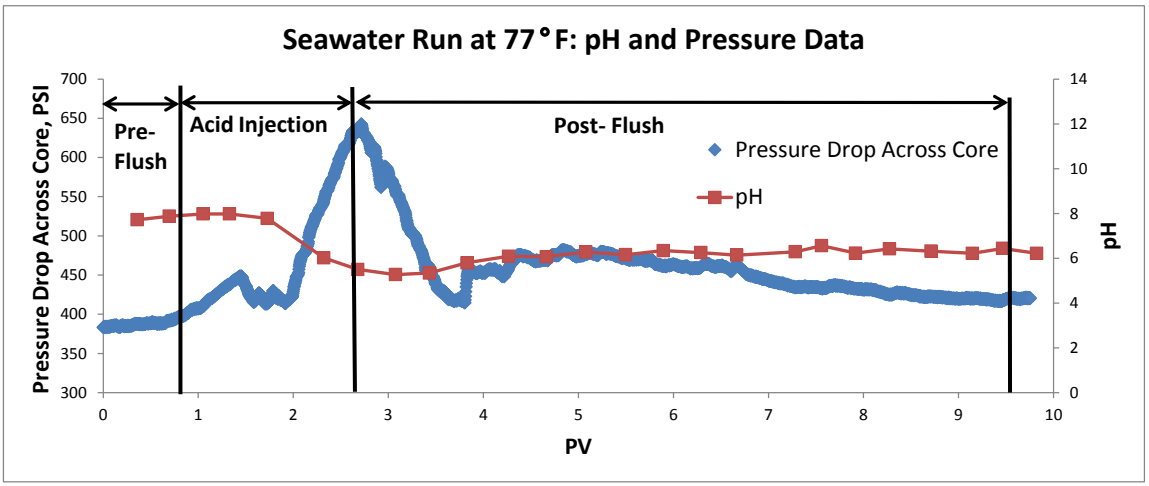

Figure 9: Graph of pressure drop across the tested core compared to the pH of the collected effluent samples for the 77°F seawater experiment.

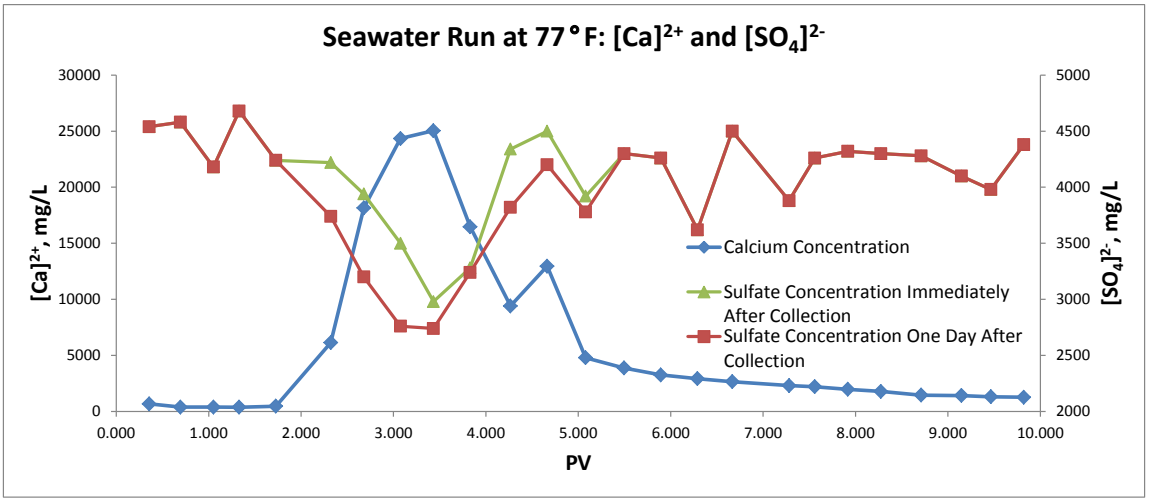

Figure 10: Graph of sulfate concentration in effluent samples measured immediately after collection and one day after collection compared to dissolved calcium concentration within collected effluent samples for the 77°F seawater experiment.

3.2.2 Temperature = 150°F

The DI water coreflood at 150°F increased the permeability within the core while not causing breakthrough. For this case a k_f/k_i ratio of 1.33 was obtained. Note that the initial permeability for this test was 3.1 mD. More stimulation is noted in this core than in the experiment with DI Water at 77°F due to the increased temperature increasing acid reactivity of the HCl. Figure 11 shows the pressure drop across the core, Figure 12 shows the comparison of pressure drop across the core to calcium and magnesium concentrations within the collected effluent samples, and Figure 13 shows a comparison of pH from the collected effluent samples to pressure drop across the core. All these graphs show that the ending condition of the core was such that no acid breakthrough occurred and no further reactions would occur within the core after the experiment. In Figure 13 there is a second drop in the pH of the collected samples after the acid

injection finished. This drop in pH suggests that live acid became trapped within a large vug during matrix acidizing and was released after DI Water was reinjected into the core.

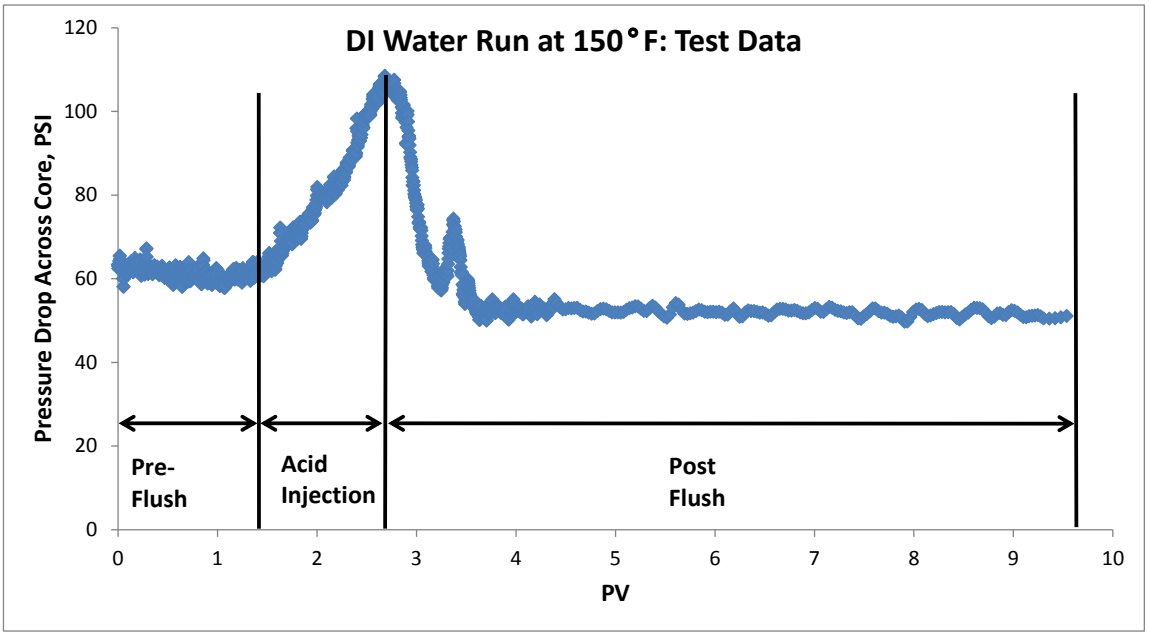

Figure 11: Graph of pressure drop across the tested core for the 150°F DI Water experiment.

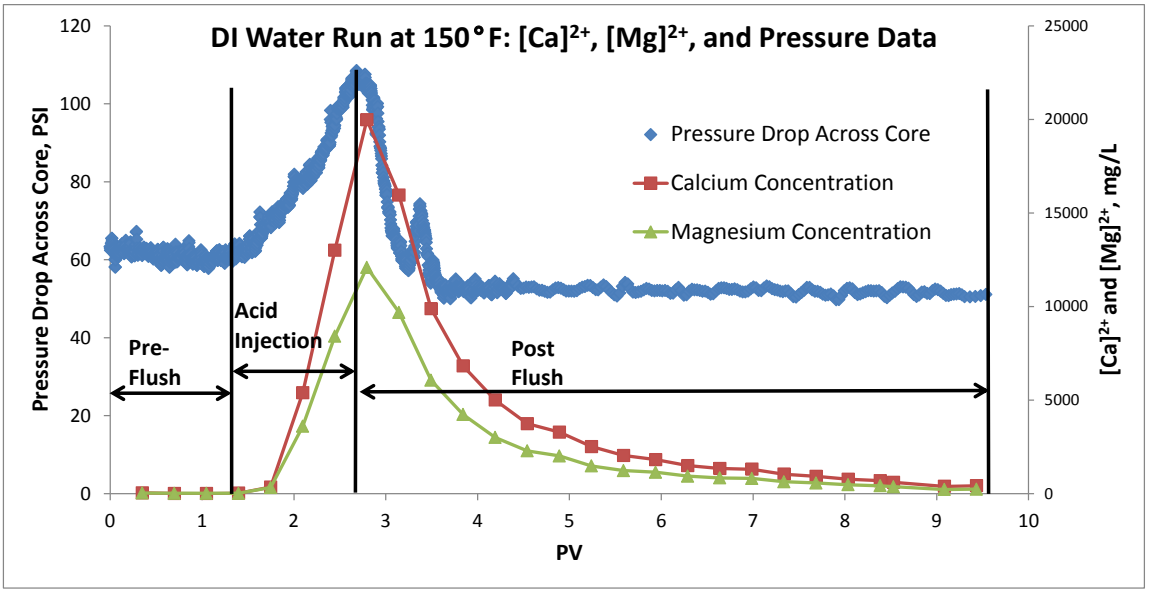

Figure 12: Graph of pressure drop across the tested core compared to dissolved calcium and magnesium concentrations within collected effluent samples for the 150°F DI Water experiment.

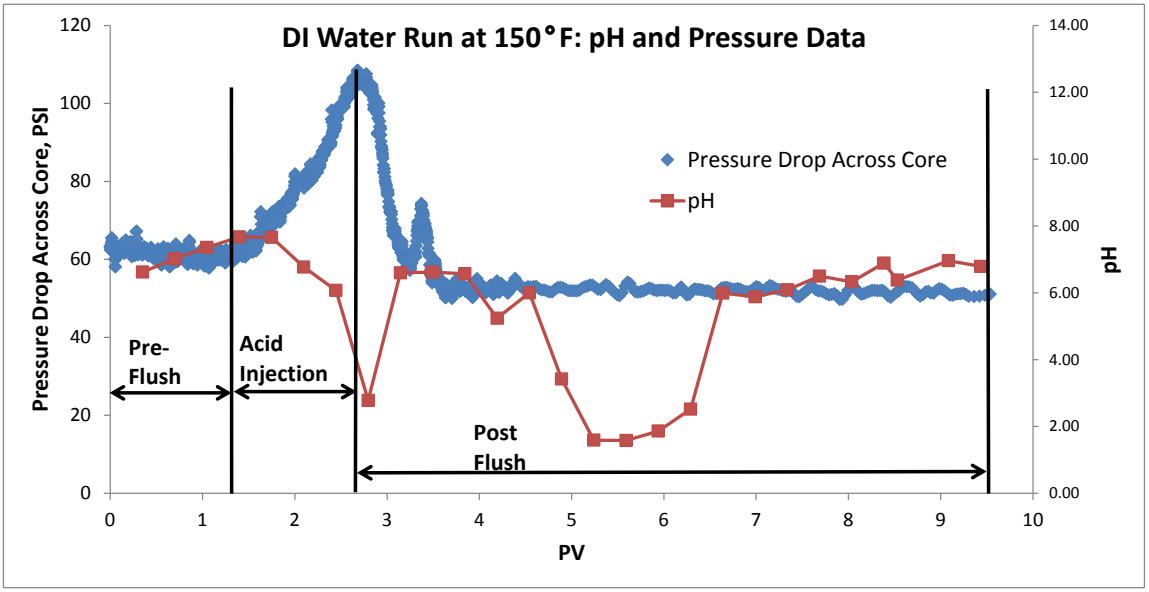

Figure 13: Graph of pressure drop across the tested core compared to the pH of the collected effluent samples for the 150°F DI Water experiment.

The coreflood using seawater and no scale inhibitors at 150°F showed large amounts of damage caused by sulfate scale formation, the k_f/k_i ratio was 0.91 for the original core with a permeability of 0.303 and the k_f/k_i ratio was 0.81 for the repeated experiment which had a core with an initial permeability of 3.39 (comparable permeability to the DI Water test run).

Figures for the first test run are as follows: Figure 14 shows the pressure drop across the original core and Figure 15 shows this for the core in the repeated coreflood. Figure 16 shows the comparison of pressure drop across the core to calcium and magnesium concentrations within the collected effluent samples and Figure 17 shows this for the core in the repeated coreflood. Figure 18 shows a comparison of pH from the collected effluent samples to pressure drop across the core and Figure 19 shows this for the core in the repeated coreflood. Figure 20 shows a comparison of sulfate concentration in collected effluent samples immediately after collection and one day after collection against calcium concentration within collected effluent samples and Figure 21 shows this for the core in the repeated coreflood. All of these graphs show that the ending condition of the core was such that no acid breakthrough occurred and no further reactions would occur within the core after the experiment.

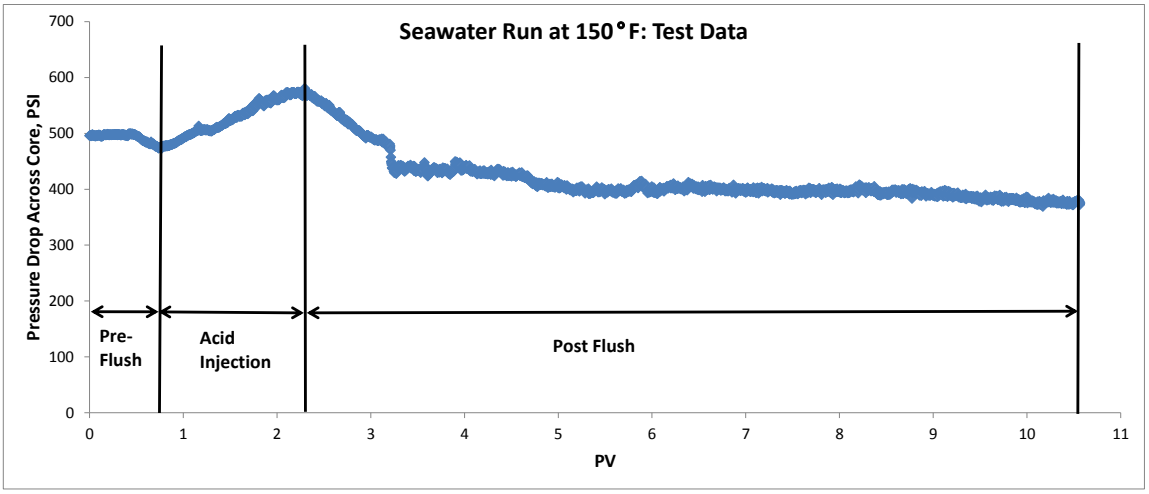

Figure 14: Graph of pressure drop across the tested core for the 150°F seawater experiment.

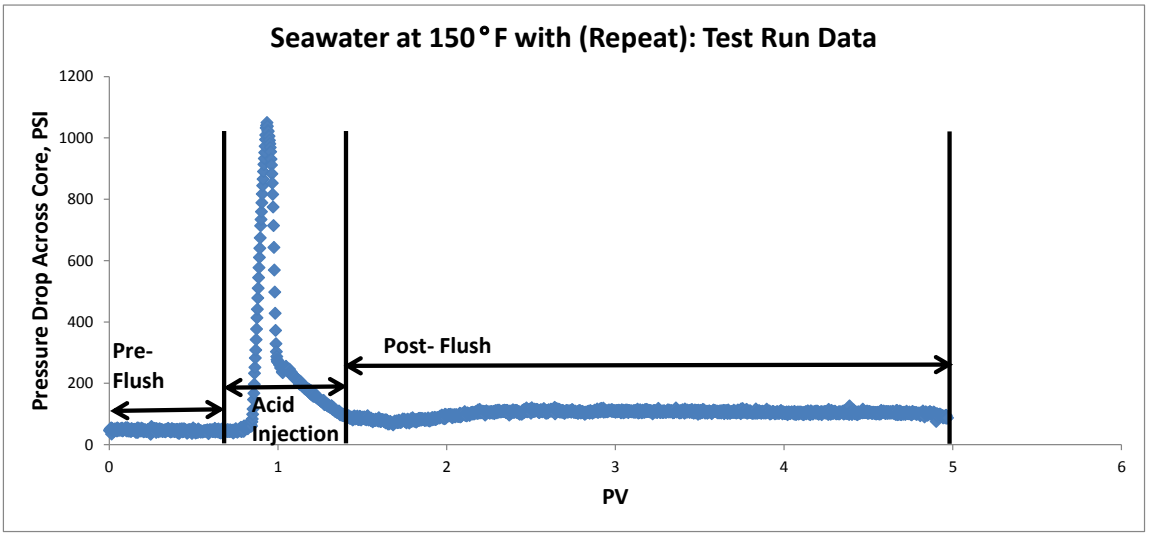

Figure 15: Graph of pressure drop across the tested core for the repeated 150°F seawater experiment.

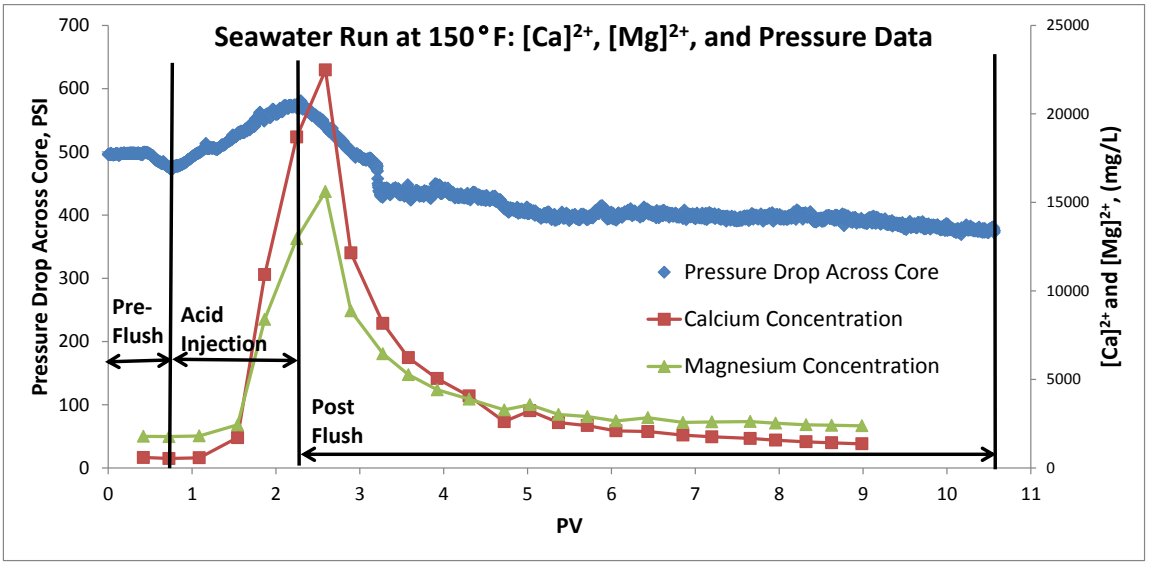

Figure 16: Graph of pressure drop across the tested core compared to dissolved calcium and magnesium concentrations within collected effluent samples for the 150°F seawater experiment.

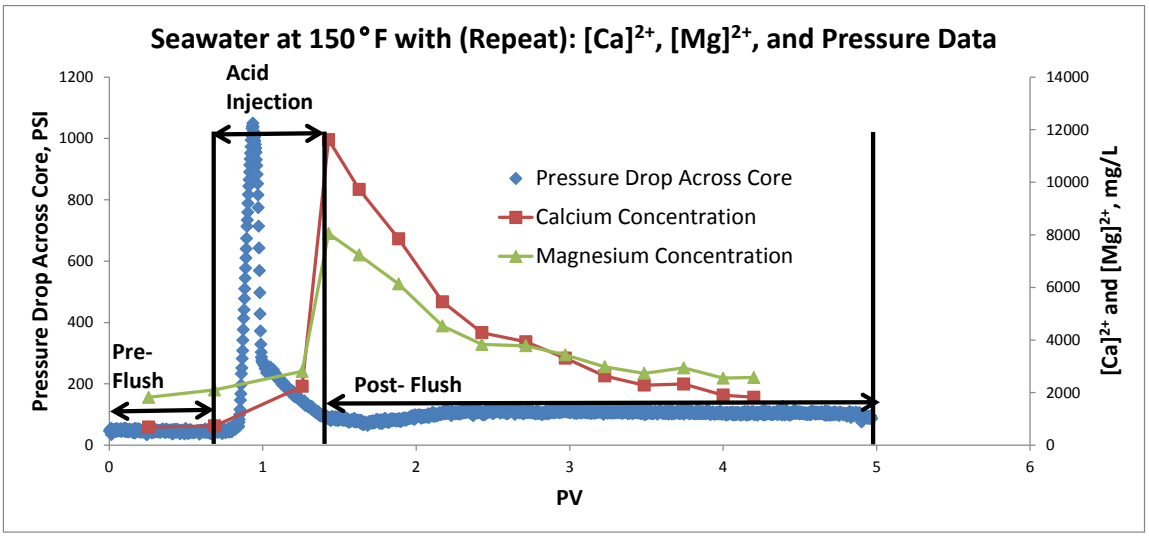

Figure 17: Graph of pressure drop across the tested core compared to dissolved calcium and magnesium concentrations within collected effluent samples for the repeated 150°F seawater experiment.

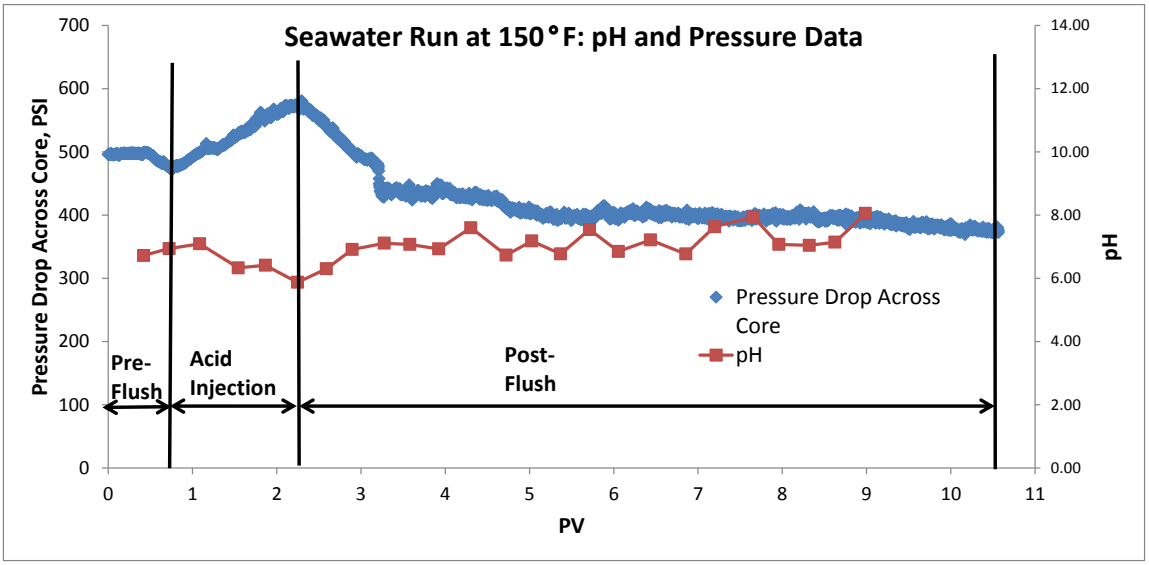

Figure 18: Graph of pressure drop across the tested core compared to the pH of the collected effluent samples for the 150°F seawater experiment.

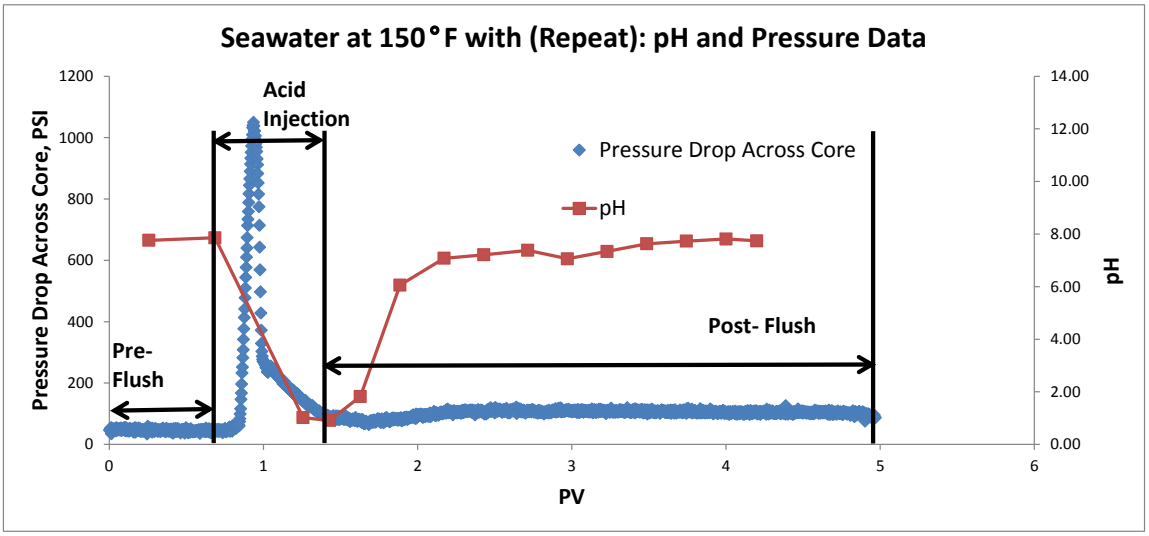

Figure 19: Graph of pressure drop across the tested core compared to the pH of the collected effluent samples for the repeated 150°F seawater experiment.

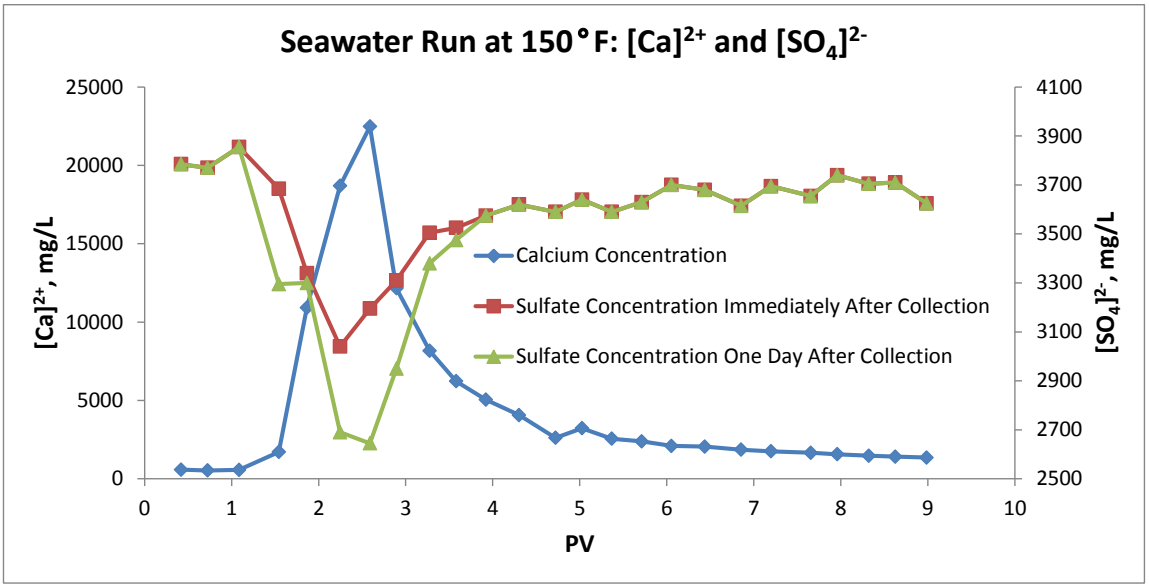

Figure 20: Graph of sulfate concentration in effluent samples measured immediately after collection and one day after collection compared to dissolved calcium concentration within collected effluent samples for the 150°F seawater experiment.

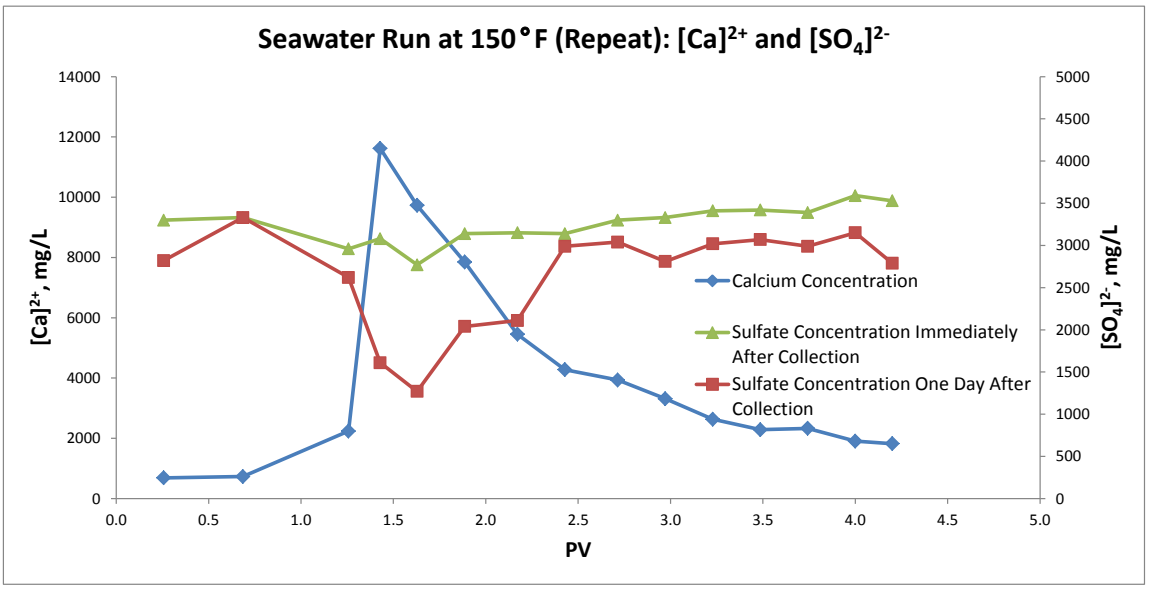

Figure 21: Graph of sulfate concentration in effluent samples measured immediately after collection and one day after collection compared to dissolved calcium concentration within collected effluent samples for the repeated 150°F seawater experiment.

3.2.3 Temperature = 250°F

The DI water coreflood at 250°F increased the permeability within the core while not causing breakthrough. Flow rate was increased at this temperature from 0.5 to 2 cc/minute to prevent face dissolution from occurring on the core when HCl was introduced. A total of 13 moles of HCl was collected within the effluent samples due to the increased flow rate, but breakthrough did not occur within the core so the experiment was considered a success. A k_f/k_i ratio of 1.31 was obtained from the experiments. Figure 22 shows the pressure drop across the core, Figure 23 shows the comparison of pressure drop across the core to calcium and magnesium concentrations within the collected effluent samples, and Figure 24 shows a comparison of pH from the collected effluent samples to pressure drop across the core. All these graphs show that the ending condition of the core and the fluid contained therein was such that no further reactions would occur within the core after the experiment and no acid breakthrough occurred during the experiment.

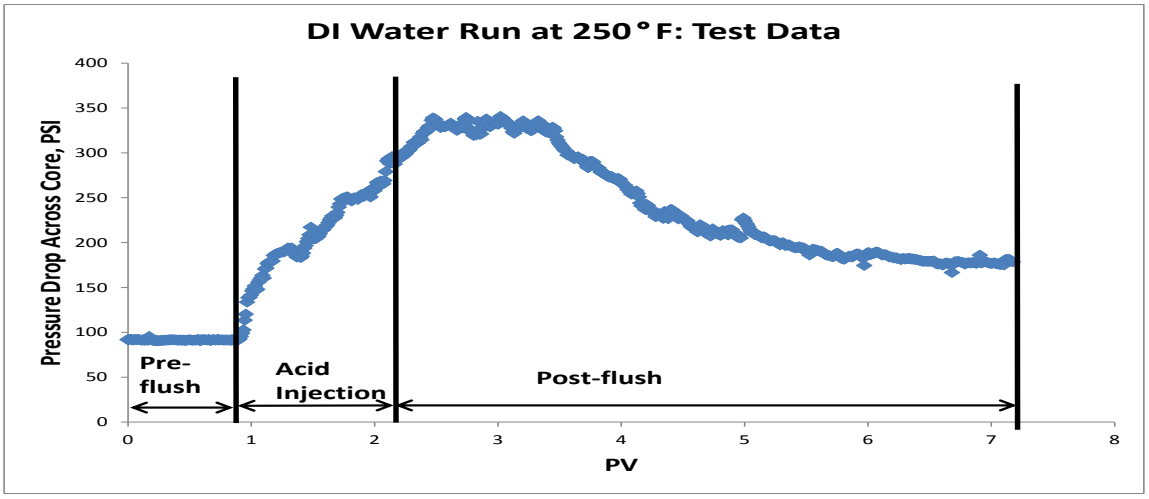

Figure 22: Graph of pressure drop across the tested core for the 250°F DI Water experiment.

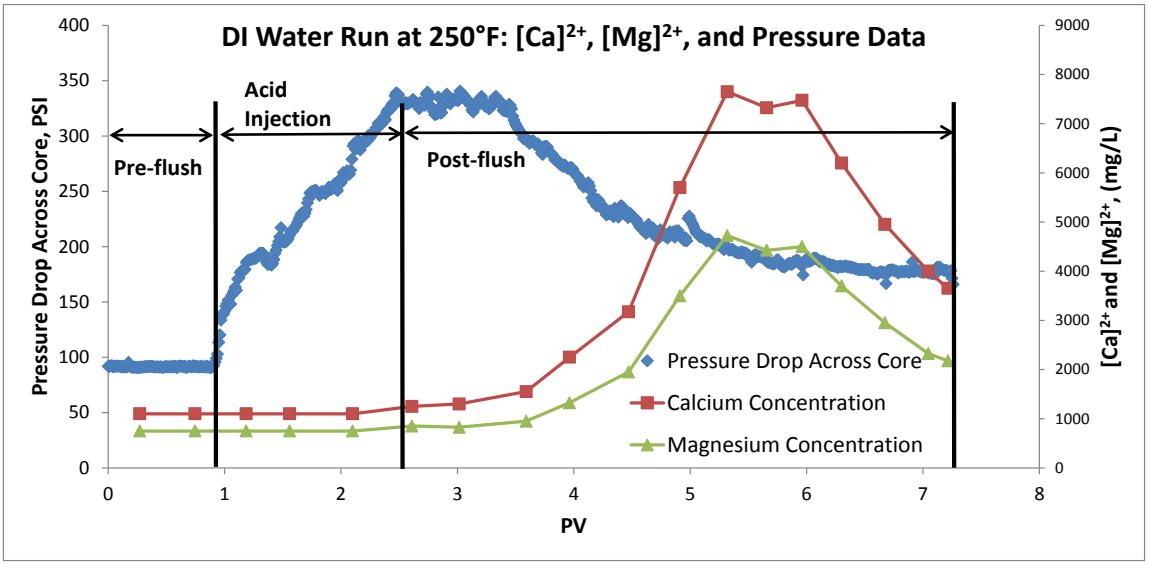

Figure 23: Graph of pressure drop across the tested core compared to dissolved calcium and magnesium concentrations within collected effluent samples for the 250°F DI Water experiment.

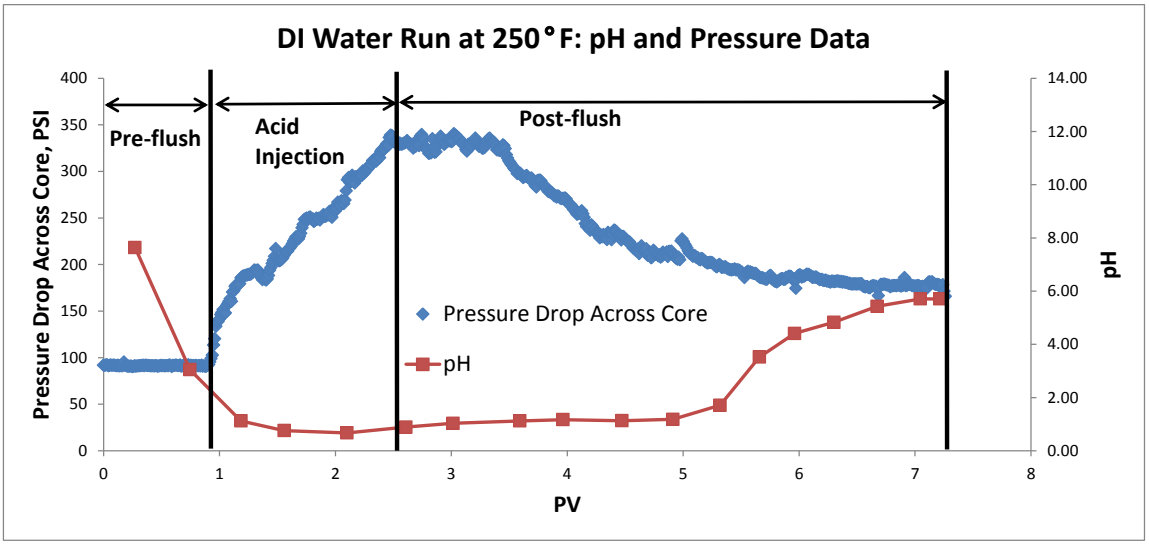

Figure 24: Graph of pressure drop across the tested core compared to the pH of the collected effluent samples for the 250°F DI Water experiment.

The coreflood using seawater and no scale inhibitors at 250°F showed large amounts of damage caused by sulfate scale formation, k_f/k_i ratio was 0.71. Figure 25 shows the pressure drop across the core, Figure 26 shows the comparison of pressure drop across the core to calcium and magnesium concentrations within the collected effluent samples, Figure 27 shows a comparison of pH from the collected effluent samples to pressure drop across the core, and Figure 28 shows a comparison of sulfate concentration in collected effluent samples immediately after collection and one day after collection against calcium concentration within collected effluent samples. All these graphs show that the ending condition of the core was such that no acid breakthrough occurred and no further reactions would occur within the core after the experiment. In this experiment the HCl fully reacted with the dolomite.

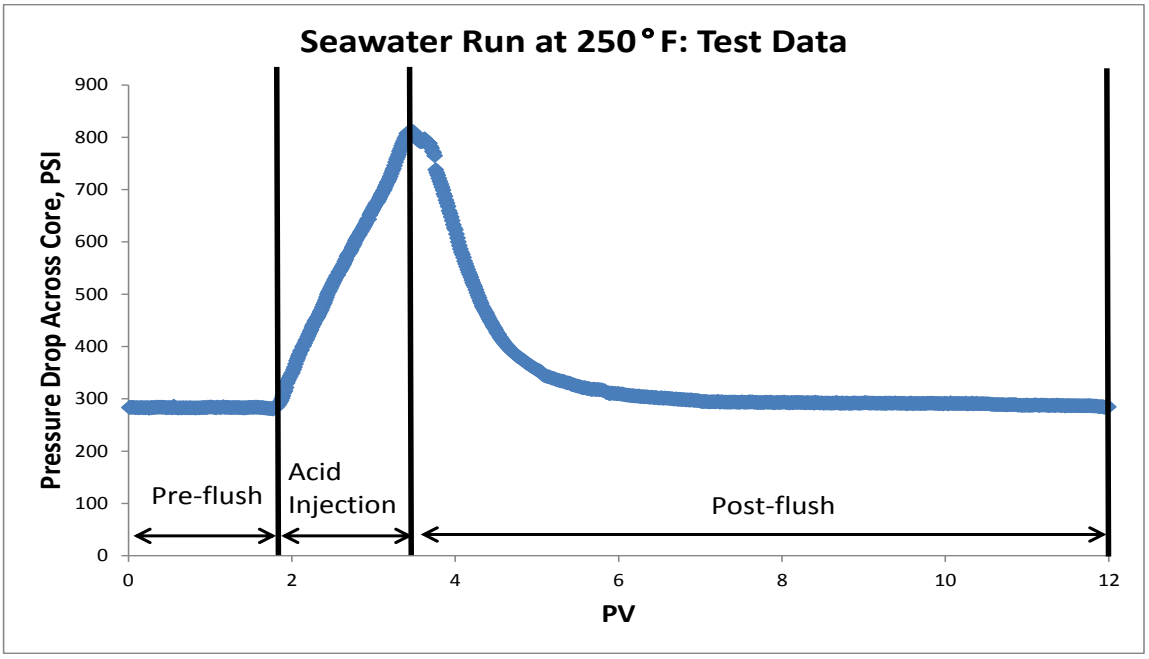

Figure 25: Graph of pressure drop across the tested core for the 250°F seawater experiment.

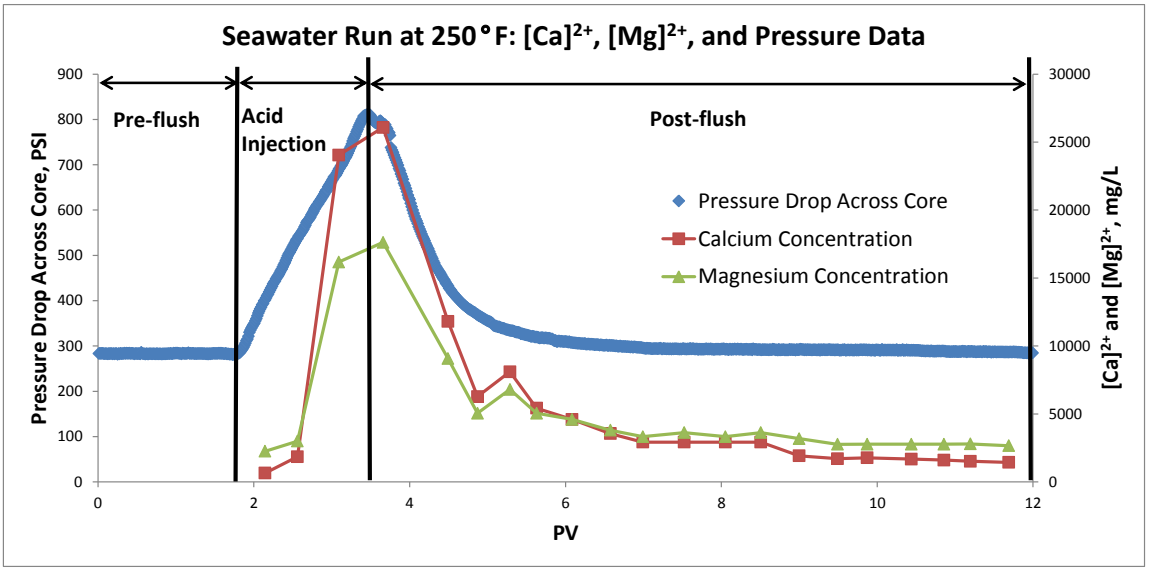

Figure 26: Graph of pressure drop across the tested core compared to dissolved calcium and magnesium concentrations within collected effluent samples for the 250°F seawater experiment.

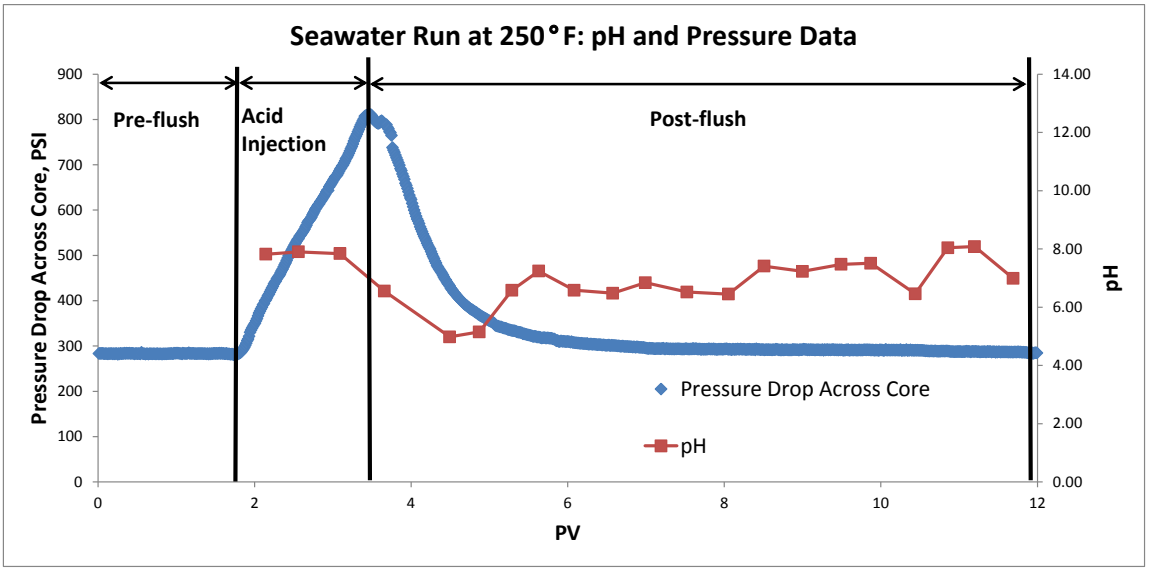

Figure 27: Graph of pressure drop across the tested core compared to the pH of the collected effluent samples for the 250°F seawater experiment.

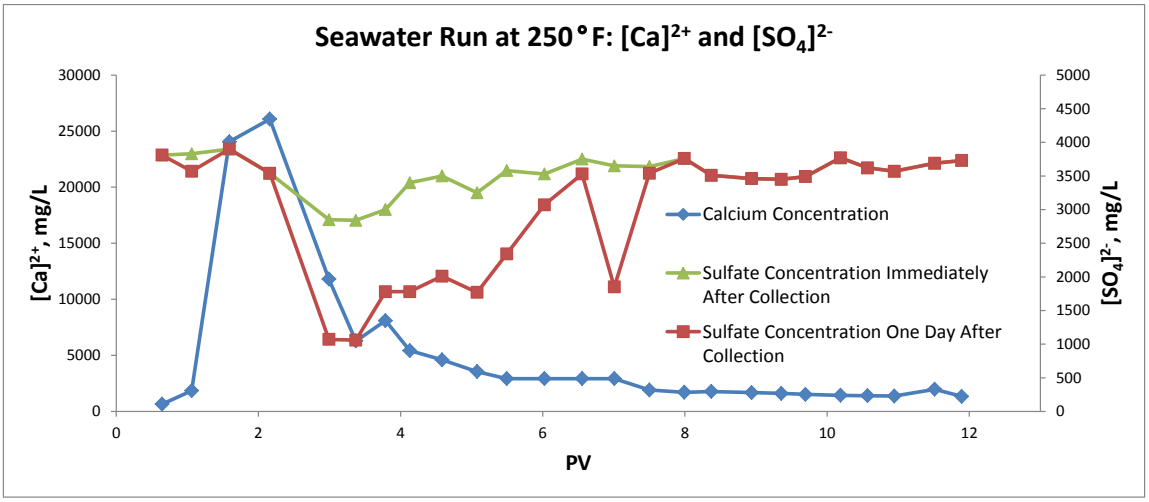

Figure 28: Graph of sulfate concentration in effluent samples measured immediately after collection and one day after collection compared to dissolved calcium concentration within collected effluent samples for the 250°F seawater experiment.

3.2.4 Temperature = 325°F

The DI water coreflood at 325°F increased the permeability within the core and caused breakthrough. The k_f/k_i ratio for this experiment was 10.89. Repeating the experiment with less HCl was unnecessary since similar results were found with the seawater case. More stimulation is noted in this core than any other case with DI Water due to the increased temperature increasing acid reactivity of the HCl. Figure 29 shows the pressure drop across the core, Figure 30 shows the comparison of pressure drop across the core to calcium and magnesium concentrations within the collected effluent samples, and Figure 31 shows a comparison of pH from the collected effluent samples to pressure drop across the core. All these graphs show that the ending condition of the core was such that no further reactions would occur within the core after the experiment and breakthrough occurred during the experiment after a very small injection of acid (about 5 mL).

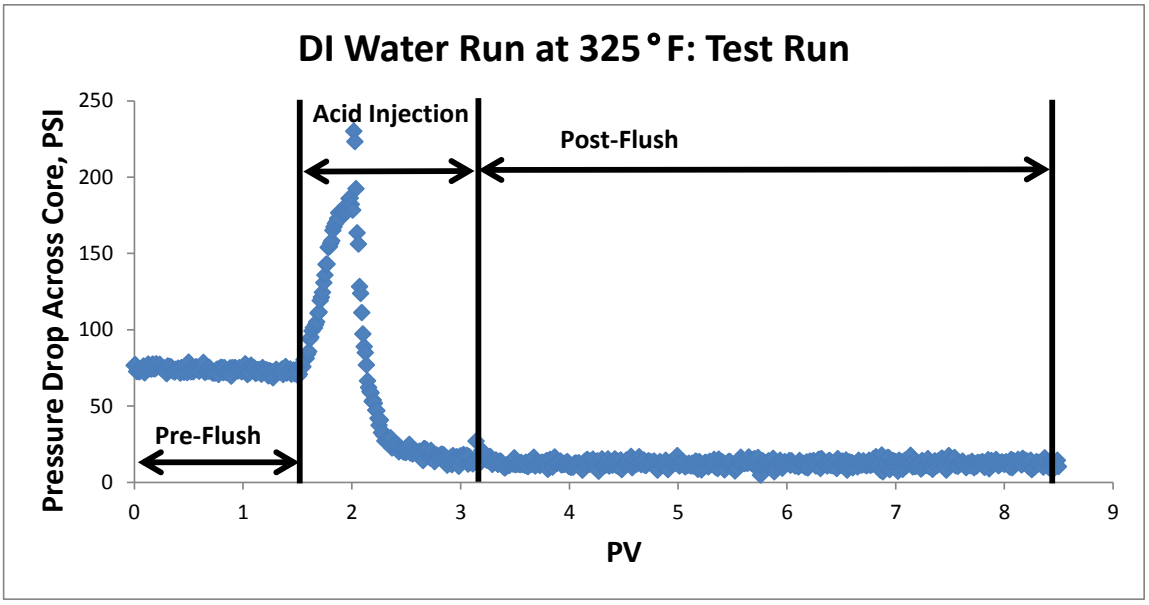

Figure 29: Graph of pressure drop across the tested core for the 325°F DI Water experiment.

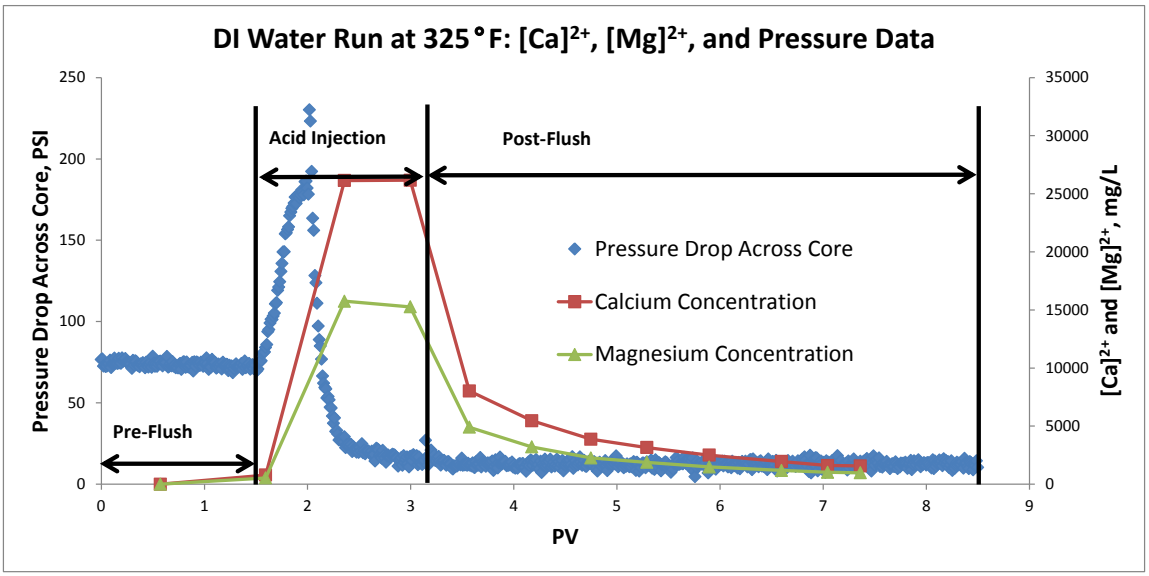

Figure 30: Graph of pressure drop across the tested core compared to dissolved calcium and magnesium concentrations within collected effluent samples for the 325°F DI Water experiment.

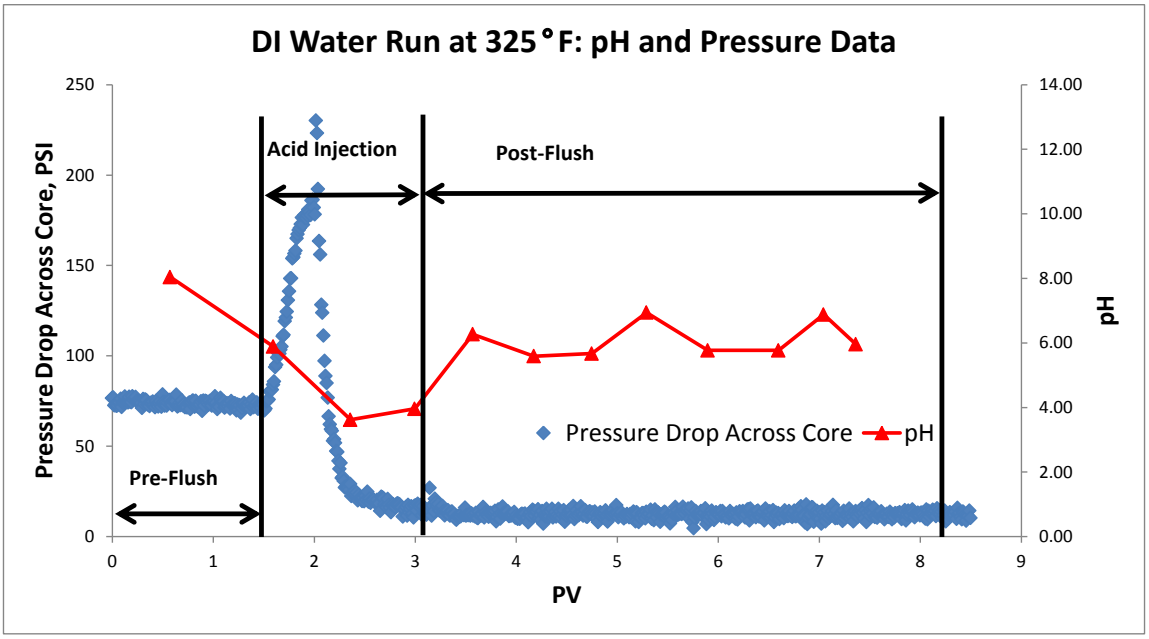

Figure 31: Graph of pressure drop across the tested core compared to the pH of the collected effluent samples for the 325°F DI Water experiment.

At 350°F, the seawater coreflood case had stimulation effects that showed breakthrough conditions after about 5 mL of HCl was injected. A large stimulation effect was noted with the k_f/k_i ratio for this experiment being 4.27. Figure 32 shows the pressure drop across the core, Figure 33 shows the comparison of pressure drop across the core to calcium and magnesium concentrations within the collected effluent samples, Figure 34 shows a comparison of pH from the collected effluent samples to pressure drop across the core, and Figure 35 shows a comparison of sulfate concentration in collected effluent samples immediately after collection and one day after collection against calcium concentration within collected effluent samples. All these graphs show that the ending condition of the core was such that no acid breakthrough occurred and no further reactions would occur within the core after the experiment. Figure 35 shows no

scale forming during the experiment, but additional scale forming after the experiment. The use of scale inhibitors at this temperature was determined to be unnecessary due to the quick breakthrough leading to under saturated conditions existing within the core during the experiment.

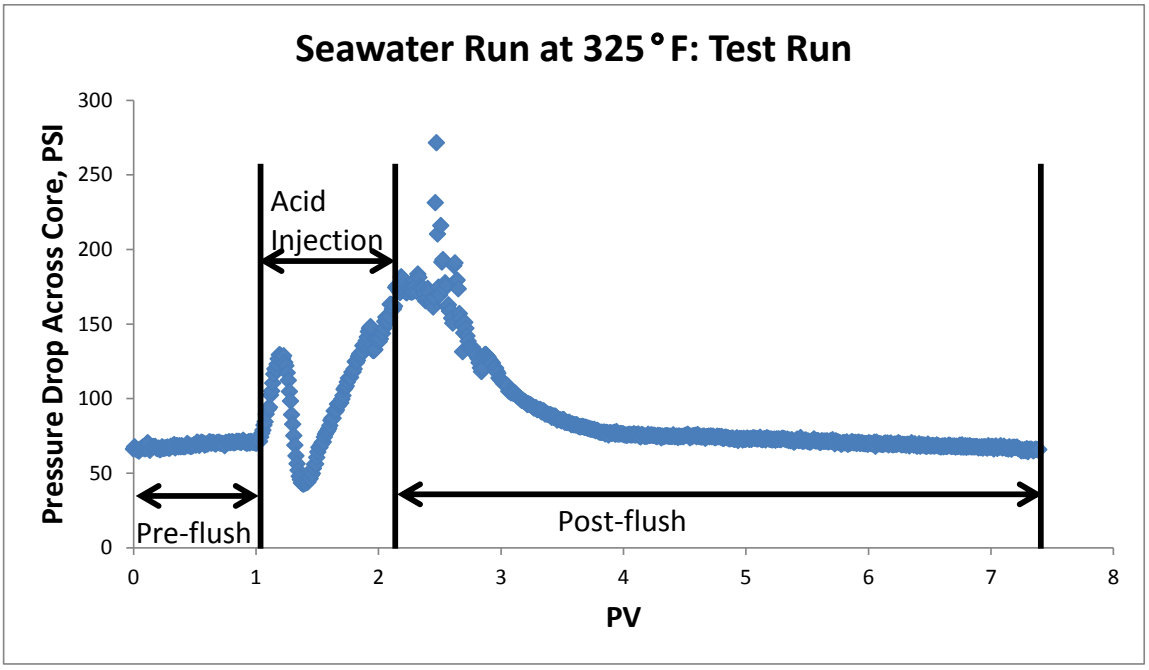

Figure 32: Graph of pressure drop across the tested core for the 325°F seawater experiment.

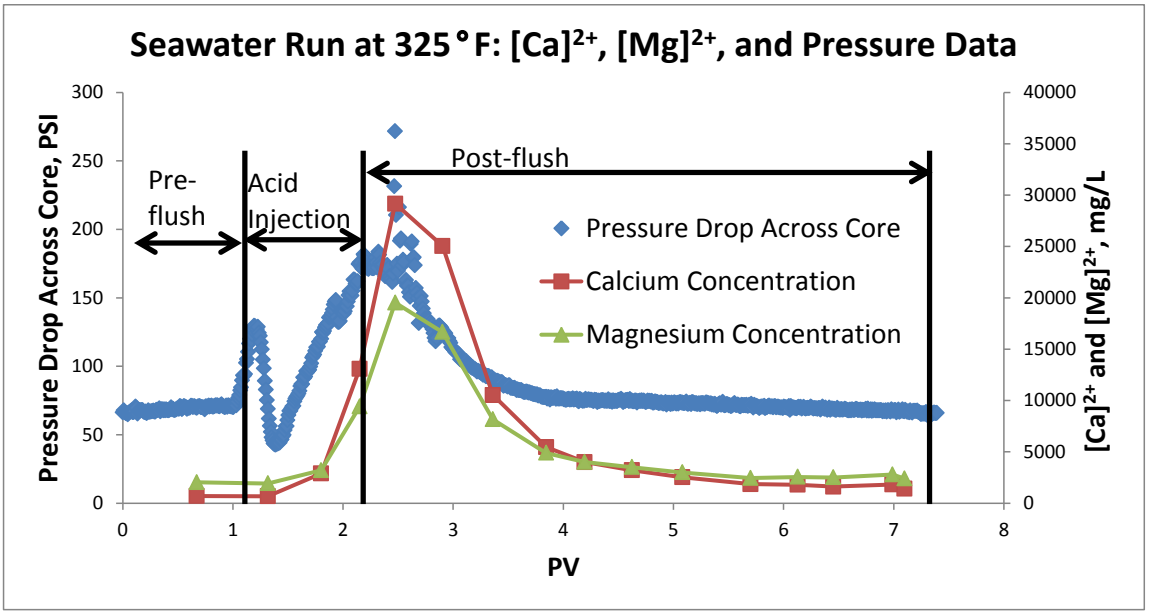

Figure 33: Graph of pressure drop across the tested core compared to dissolved calcium and magnesium concentrations within collected effluent samples for the 325°F seawater experiment.

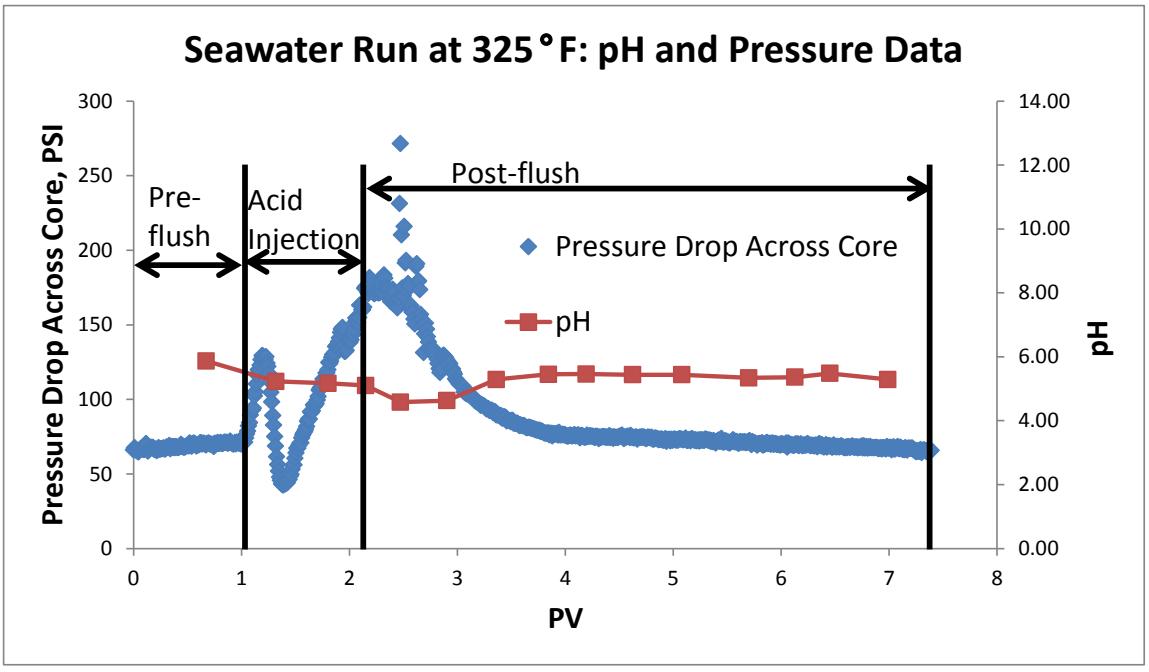

Figure 34: Graph of pressure drop across the tested core compared to the pH of the collected effluent samples for the 325°F seawater experiment.

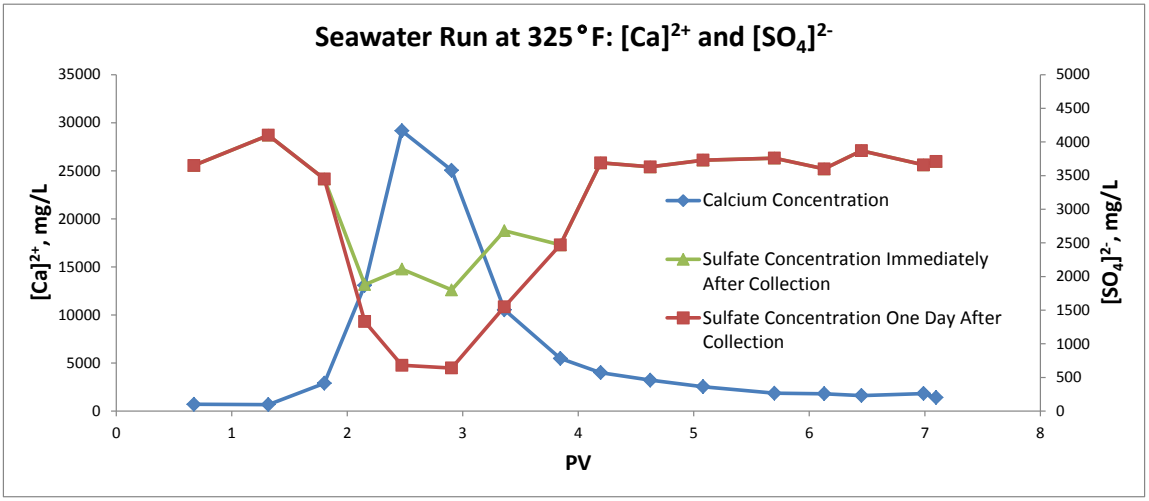

Figure 35: Graph of sulfate concentration in effluent samples measured immediately after collection and one day after collection compared to the dissolved calcium concentration within collected effluent samples for the 325°F seawater experiment.

3.3 Discussion

Calcium sulfate scale will damage dolomite formations acidized by HCl at temperatures up to 250°F. Table 4 summarizes the initial and final conditions of the experiments conducted without scale inhibitors and shows that all acidized cores saturated with seawater at 250°F and below experienced reductions in permeability throughout the experiment. The table shows a clear trend of seawater always having less of a stimulation effect than the DI Water counterparts, even above 250°F. At 325°F the acid reaction occurs so quickly that breakthrough can be achieved with a significantly lower volume of acid, which in turn would lower the concentration of free calcium and magnesium ions. The scale that did form during this experiment formed slower than the growth of the wormholes which allowed stimulation to occur even though scale did

form. For these reasons, it was determined that scale inhibitors will be needed for temperatures up to 250°F.

Table 5 shows the amount of sulfate precipitated and the amount of calcium and magnesium dissolved in each experiment. During the repeat test at 150°F, it was observed that more damage occurred in the higher permeability core and more scale precipitated within the same core. This follows the observations of Moghadasi et al. (2004). The total amount of sulfate which precipitated increased during the experiments as the temperature increased. This additional precipitation is caused by the solubility of calcium sulfate decreasing as temperature increases.

Table 4: Table summarizing initial and final core conditions along with flow rate.

		Porosity (%)	PV (cc)	k-initial (mD)	k-final (mD)	kf/ki	Flow Rate (cc/min)
77F	DI Water	8.5	14.76	0.819	0.935	1.14	0.5
	Seawater	7.3	12.6	0.42	0.39	0.93	0.5
150F	DI Water	8.2	14.31	2.339	3.1	1.33	0.5
	Seawater	10.07	17.5	3.39	2.74	0.81	0.5
	Seawater	7.6	13.13	0.303	0.28	0.92	0.5
250F	DI Water	9.3	16.16	0.78	1.02	1.31	2
	Seawater	7.6	13.2	2.18	1.55	0.71	2
325F	DI Water	9.02	15.69	1.18	13	10.89	2
	DI Water	13	21.1	1.204	110	91.36	2
	Seawater	15.8	25.6	1.187	5.07	4.27	2

Table 5: Table summarizing the amount of precipitated sulfate during each test and dissolved calcium and magnesium.

	77F	150F	250F	325F
Total Sulfate Injected, mg	568	463	611	513
Total Sulfate Ejected, mg	509	424	563	434
Total Sulfate After One Day, mg	492	415	472	403
Sulfate Precipitated in Core, mg	59	39	48	78
Addition Sulfate Precipitation After One Day, mg	18	9	91	31
Total Sulfate Precipitated, mg	76	48	139	109
Total Dissolved Calcium, mg	763	415	758	678
Total Dissolved Magnesium, mg	690	432	787	782

4. MITIGATING DAMAGE DUE TO CALCIUM SULFATE SCALE

4.1 Introduction

Scale inhibitors operate with two main modes of inhibition: nucleation inhibition and crystal growth inhibition. Nucleation inhibition is the process of preventing scales from creating crystal seeds. Crystal growth inhibition is the process of preventing scale crystals from increasing in in size. All scale inhibitors work using both types of inhibition mechanisms, though one mechanism is typically favored over the other [4]. Polymer based scale inhibitors generally favor nucleation inhibition, and short chain scale inhibitors generally favor crystal growth inhibition. Nucleation inhibition is less well understood than crystal growth inhibition and is thought to work by bonding with accumulating scale forming ions and disrupting the ion cluster causing ions to disperse before they form scale on a solid surface; then the inhibitor is released when ion cluster breaks apart allowing the scale inhibitor to disrupt more clusters. Scale inhibitors can also benefit from the dispersion effect inherent in some scale inhibitors. Crystal growth inhibition works by the scale inhibitor adsorbing onto existing scale crystal structures and preventing further growth of the crystal and by adsorbing onto scale precipitates within the bulk solution to prevent the scale from depositing on the wall. Both types of scale inhibitors can be used in squeeze treatments where the scale inhibitor is injected into the reservoir and expected to prevent scale growth for the life of the scale inhibitor [14].

DTPMP (Diethylene Triamine Penta (Methylene Phosphonic acid)) is a short chain phosphonate based scale inhibitor which acts like a chelating agent and favors crystal growth inhibition. It is one of the oldest phosphonate based scale inhibitors to be used in the oil field. This scale inhibitor performs well at high temperatures compared to other short chain based scale inhibitors and has long retention rates within the reservoir which make it suitable for squeeze treatments[15]. The phosphonic acid group within the scale inhibitor is the active group and does not perform well in environments with pH values greater than 7[16].

BHMT (Bis(HexaMethylene Triamine penta (methylene phosphonic acid))) is another short chain phosphonate based scale inhibitor which acts like a chelating agent and favors crystal growth inhibition. This scale inhibitor performs well in high pH conditions, but does not perform well at high temperatures[17], unlike DTPMP. Increasing the Ca^{2+} concentration will increase the inhibitor efficiency, but can lead to calcium phosphonate precipitation, especially in the presence of iron[18]

Sulfonated polymer is a long chain polymer based scale inhibitor which prefers nucleation inhibition. It is known to work well at low temperatures and high supersaturation conditions[19], which is a problem for many phosphonate based scale inhibitors. These scale inhibitors can also be designed for applications above 350°F. Calcium, magnesium, and iron ions do not affect this type of scale inhibitor as much as they do for crystal growth inhibition type scale inhibitors[4].

P-tagged sulfonated polymer is a long chain polymer based scale inhibitor which prefers nucleation inhibition. It is another type of sulfonated polymer with phosphorous

included in the molecular chain. The scale inhibitor behaves similarly to sulfonated polymer.

PAA (PolyAcrylic Acid) is a scale inhibitor which favors crystal growth inhibition. It performs better as pH increases, due to increasing dissociation of the carboxylic groups at increasing pH values, increasing the affinity for PAA to absorb onto the scale crystal surface [20].

PPCA (Phosphino-PolyCarboxylic Acid) is a short chain phosphonate based scale inhibitor which has a balance of crystal growth inhibition and nucleation inhibition mechanisms. The effect of divalent ions is less than that observed on DTPMP [19, 21]. PPCA inhibition efficiency increases with increasing temperature and decreases at low temperatures, though it does not lose as much inhibition efficiency as DTPMP [4].

4.2 Results

In an acidic environment (conditions created to simulate conditions where 15 wt% HCl reacts with dolomite and 1 wt% HCl remains) DTPMP and BHMT were effective at any concentration; and sulfonated polymer and P-tagged sulfonated polymer were effective at 150 ppm and 10,000 ppm. Polyacrylic acid and PPCA were not effective scale inhibitors at any inhibitor concentration. According to He et al (2013) scale inhibitors will be least effective during the 1 wt% partially spent HCl condition during matrix acidizing. Table 6 shows the overall results from the static jar tests.

Table 6: Results of static jar tests. The cells highlighted in red indicate scale inhibitor failed the test at the specified concentration, and cells highlighted green indicate that the test passed at the specified conditions.

	Spent Acid/Scale Inhibitor (SI) System															Good
	50 ppm			150 ppm			500 ppm			1000 ppm			10000 ppm			Bad
SI	RT	150F	210F	RT	150F	210F	RT	150F	210F	RT	150F	210F	RT	150F	210F	
PPCA	LC	ThP	ThP	N	C	P	SC	ThP	ThP	C	ThP	ThP	C	ThP	ThP	N = Solution is Clear
Polyacrylic Acid	SC	P	P	SC	ThP	ThP	SC	ThP	ThP	C	ThP	ThP	C	P	C	C = Solution is Cloudy
Sulfonated Polymer	C	ThP	P	N	tP	tP	SC	P	tP	C	C/P	P	C	N	N	SC = Severely Cloudy
DTPMP	C	tP	tP	LC	LC	tP	N	LC	tP	N	N	N	N	N	N	LC = Lightly Cloudy
BHMT	N	LC	tP	LC	LC	tP	N	LC	tP	N	LC	tP	N	N	N	P = Precipitation Layer Formed
P-Tagged Sulfonated Polymer	C	ThP	ThP	N	N	N	SC	P	P	C	P	P	N	N	N	ThP = Thick Precipitation Layer
No SI	LC	C	P													tP = Thin Precipitation

Table 7 shows pictures taken of the synthetic spent acid environments for samples tested with 150 ppm scale inhibitor and no scale inhibitor. PPCA and polyacrylic acid showed signs of enhanced scale precipitation during static jar tests at 150 ppm. DTPMP, BHMT, and P-tagged sulfonated polymer work as sulfate scale inhibitors for acidizing dolomite under idealized conditions. The corefloods with scale inhibitors following the results of the static jars tests were conducted at 150 ppm of each passing scale inhibitor.

Table 7: Pictures of samples at the end of the static jar tests with 150 ppm of each scale inhibitor.

	150 ppm of Scale Inhibitor						
Temperature	No Scale Inhibitor	PPCA	Polyacrylic Acid	Sulfonated Polymer	DTPMP	BHMT	P-tagged sulfonated polymer
77°F	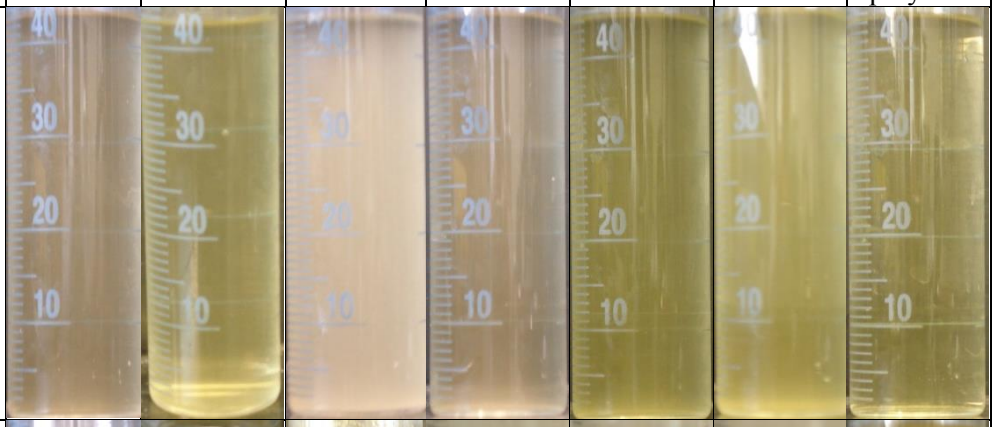						
150°F	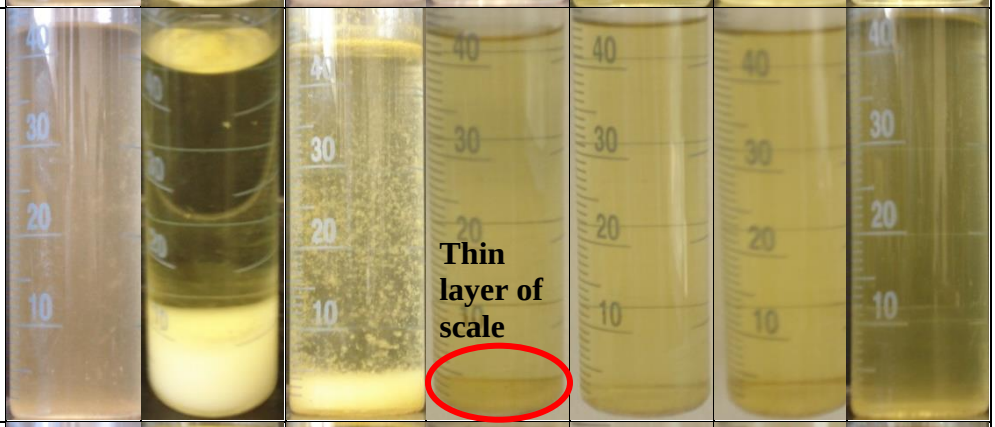			Thin layer of scale			
210°F	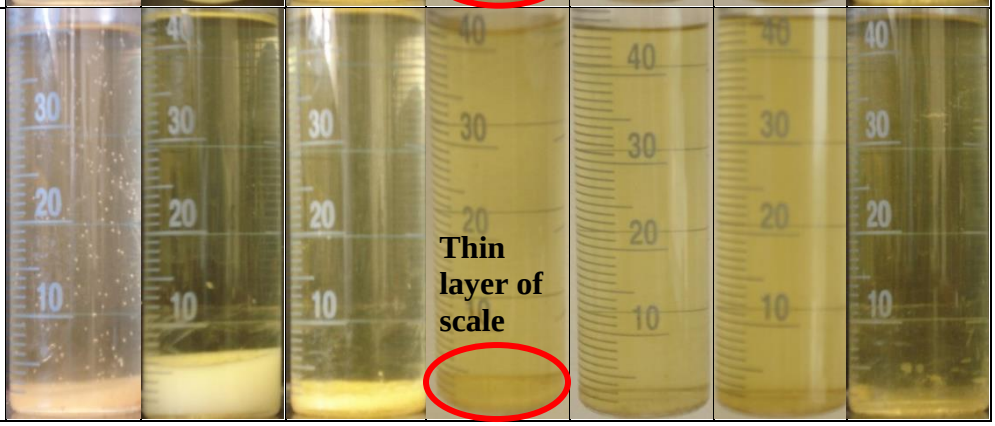			Thin layer of scale			

4.2.1 BHMT

The coreflood with BHMT and seawater at 150°F had more scale formation during the coreflood than the case with seawater alone. SEM analysis of precipitate collected in effluent samples showed the precipitate was a calcium phosphonate scale. This was caused by iron within the core reacting with phosphonate in the scale inhibitor to create a layer of iron phosphonate scale on the surface of the core along with the calcium sulfate that formed after the scale inhibitor finished interacting with the iron. Damage caused by the addition of BHMT during the experiment can be seen by the k_f/k_i ratio which was 0.78. The other corefloods at different temperatures were not conducted because the iron phosphonate precipitation would occur at the other temperatures being tested. Figure 36 shows the pressure drop across the core, Figure 37 shows the comparison of pressure drop across the core to calcium and magnesium concentrations within the collected effluent samples, Figure 38 shows a comparison of pH from the collected effluent samples to pressure drop across the core, and Figure 39 shows a comparison of sulfate concentration in collected effluent samples immediately after collection and one day after collection against the calcium concentration within collected effluent samples. All these graphs show that the ending condition of the core was such that no acid breakthrough occurred and no further reactions would occur within the core after the experiment.

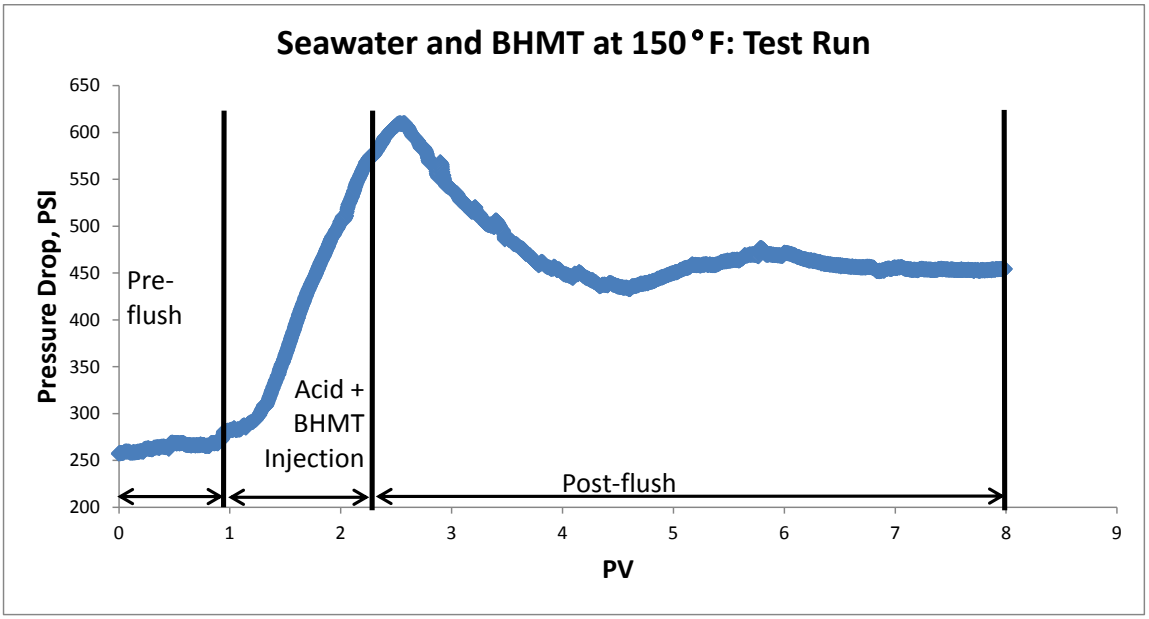

Figure 36: Graph of pressure drop across the tested core for the 150°F seawater and 150 ppm BHMT experiment.

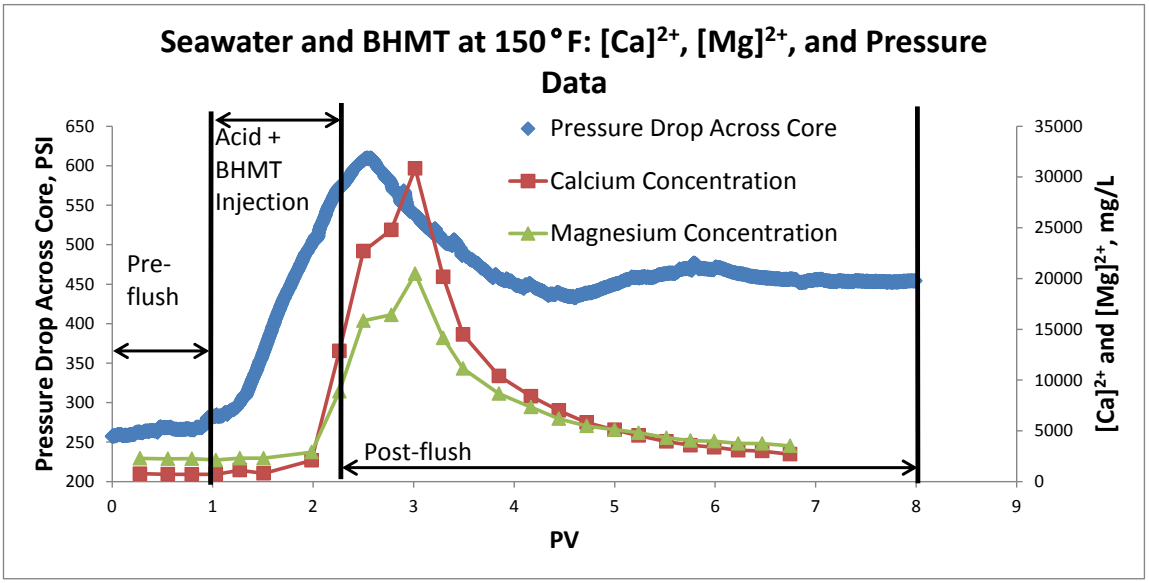

Figure 37: Graph of pressure drop across the tested core compared to dissolved calcium and magnesium concentrations within collected effluent samples for the 150°F seawater and 150 ppm BHMT experiment.

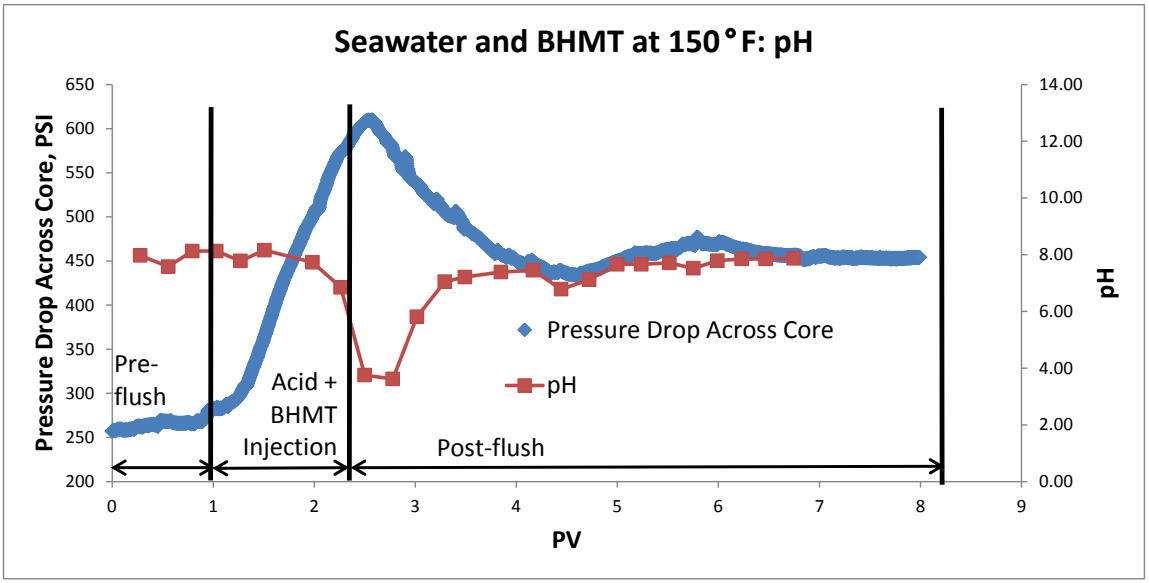

Figure 38: Graph of pressure drop across the tested core compared to the pH of the collected effluent samples for the 150°F seawater and 150 ppm BHMT experiment.

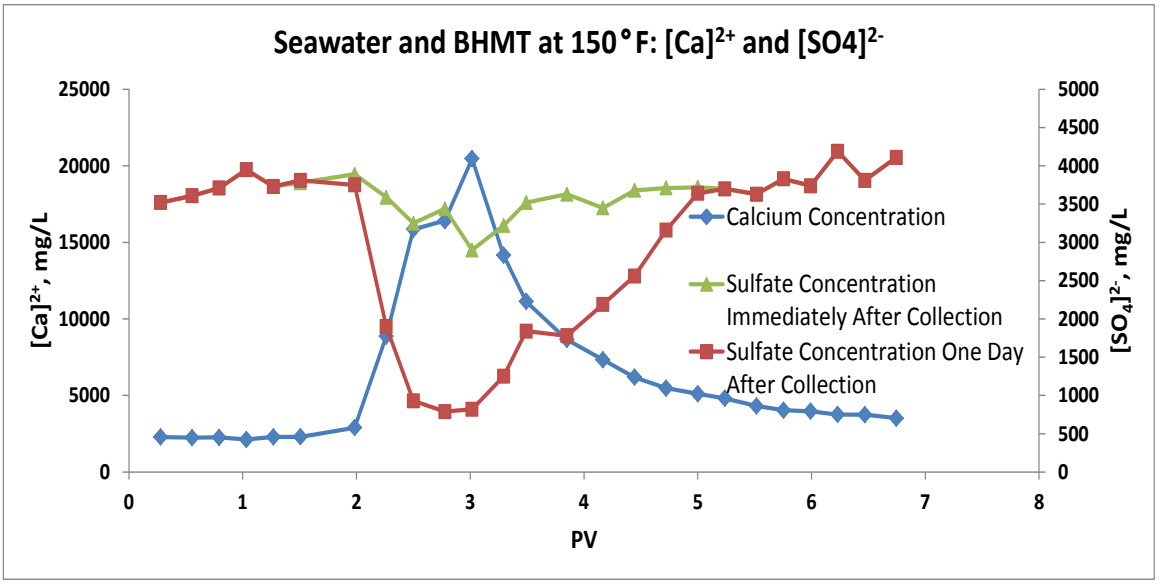

Figure 39: Graph of sulfate concentration in effluent samples measured immediately after collection and one day after collection compared to dissolved calcium concentration within collected effluent samples for the 150°F seawater and 150 ppm BHMT experiment.

4.2.2 P-Tagged Sulfonated Polymer

At 77°F the P-tagged sulfonated polymer showed signs of damage as seen by the k_f/k_i ratio of 0.43. This was caused by the large polymer chains of the scale inhibitor becoming trapped within tight pore throats within the dolomite core. Less sulfate scale formed during the coreflood with the scale inhibitor than in the coreflood without the scale inhibitor, but after the coreflood an increased amount of sulfate scale formed. The total amount of scale formed during the 77°F tests (during the coreflood and additional precipitation after) with and without the scale inhibitor were the same which indicates that the scale inhibitor became trapped within the core and was not present in the collected samples. Figure 40 shows the pressure drop across the core, Figure 41 shows the comparison of pressure drop across the core to calcium and magnesium concentrations within the collected effluent samples, Figure 42 shows a comparison of pH from the collected effluent samples to pressure drop across the core, and Figure 43 shows a comparison of sulfate concentration in collected effluent sample immediately after collection and one day after collection against calcium concentration within collected effluent samples. All these graphs show that the ending condition of the core was such that no further reactions would occur within the core after the experiment and no acid breakthrough occurred during the experiment.

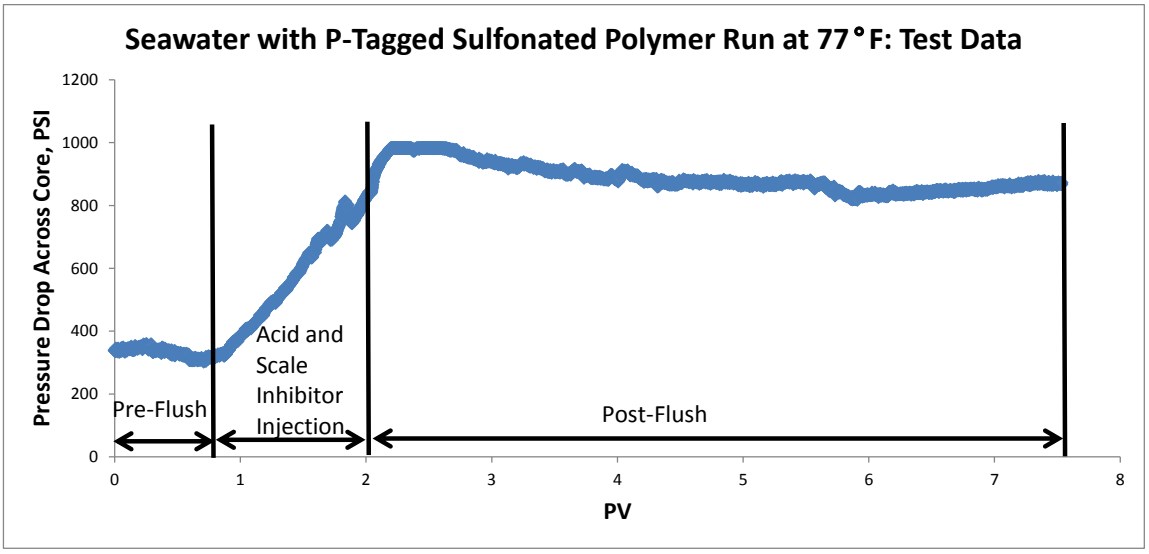

Figure 40: Graph of pressure drop across the tested core for the 77°F seawater and 150 ppm P-tagged sulfonated polymer experiment.

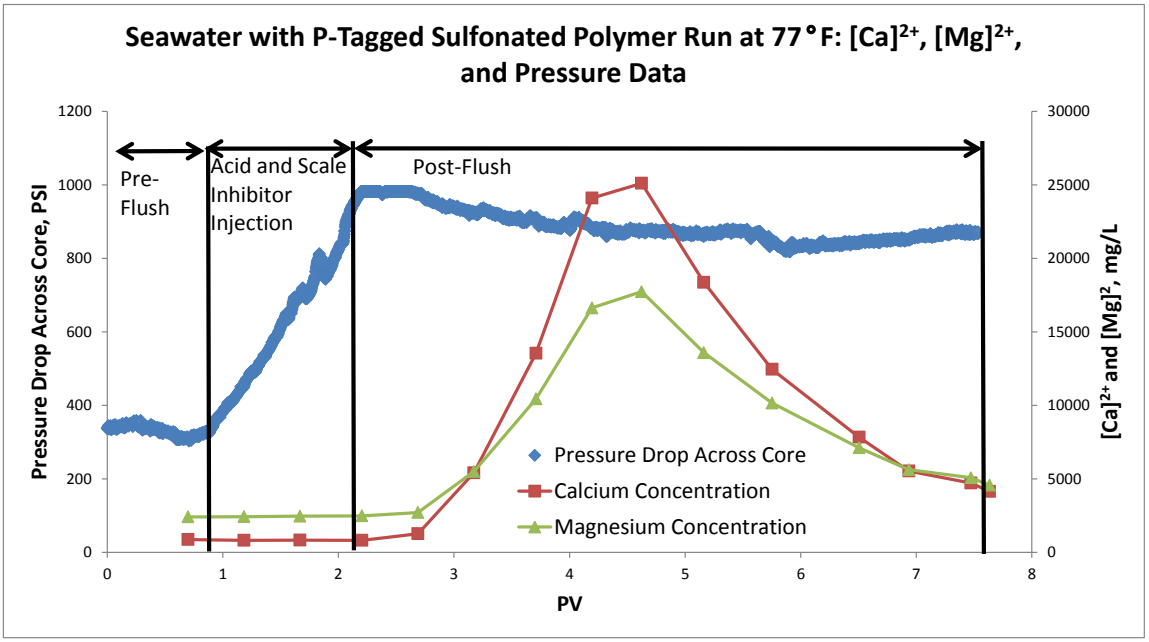

Figure 41: Graph of pressure drop across the tested core compared to dissolved calcium and magnesium concentrations within collected effluent samples for the 77°F seawater and 150 ppm P-tagged sulfonated polymer experiment.

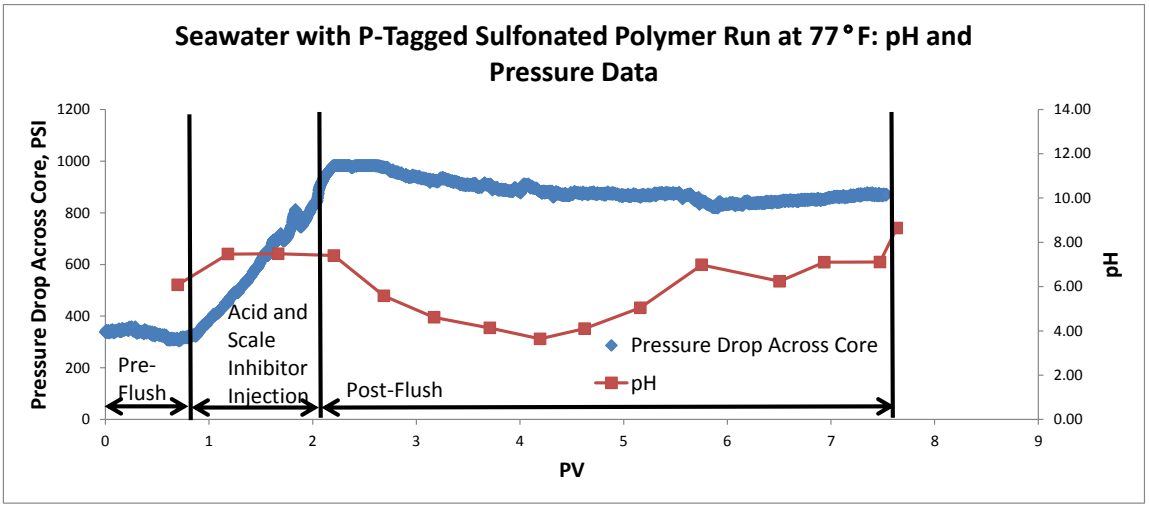

Figure 42: Graph of pressure drop across the tested core compared to the pH of the collected effluent samples for the 77°F seawater and 150 ppm P-tagged sulfonated polymer experiment.

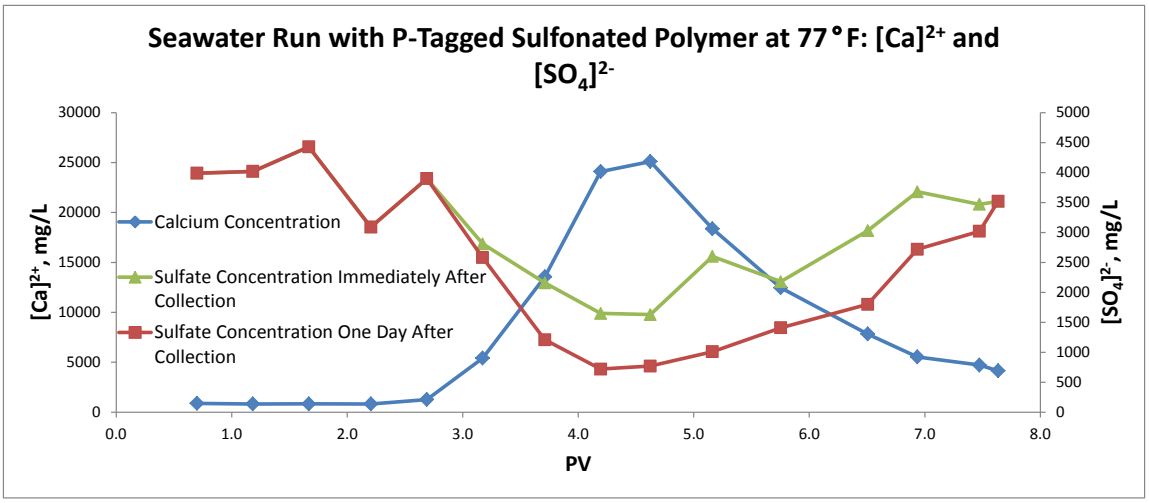

Figure 43: Graph of sulfate concentration in effluent samples measured immediately after collection and one day after collection compared to dissolved calcium concentration within collected effluent samples for the 77°F seawater and 150 ppm P-tagged sulfonated polymer experiment.

The test at 250°F with P-tagged sulfonated polymer showed that less damage formed when scale inhibitors were added to the acid treatment at 250°F than when no scale inhibitor was added. The k_f/k_i ratio was 1.01, which shows that the permeability of the core remained unchanged. This reduction in damage compared to the seawater case with no scale inhibitors at 250°F shows that the scale inhibitor works in its basic function reducing scale formation, but the large polymer chains prevent this scale inhibitor from being fully effective in cores within the permeability range that was tested in these experiments. Figure 44 shows the pressure drop across the core, Figure 45 shows the comparison of pressure drop across the core to calcium and magnesium concentrations within the collected effluent samples, Figure 46 shows a comparison of pH from the collected effluent samples to pressure drop across the core, and Figure 47 shows a comparison of sulfate concentration in collected effluent samples immediately after collection and one day after collection against calcium concentration within collected effluent samples. All these graphs show that the ending condition of the core was such that no acid breakthrough occurred and no further reactions would occur within the core after the experiment.

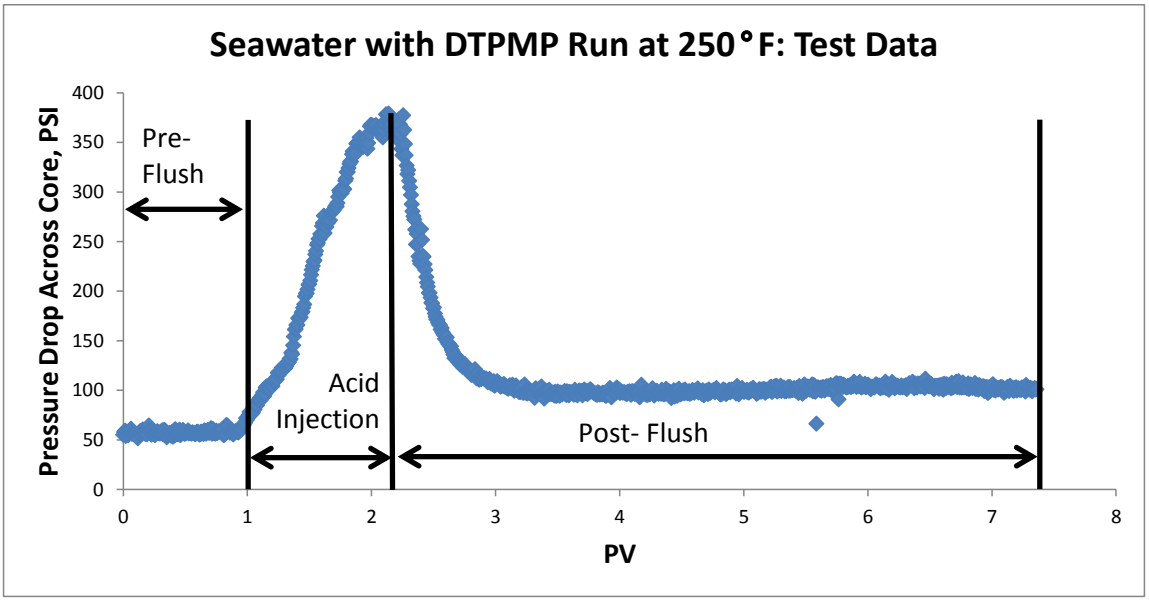

Figure 44: Graph of pressure drop across the tested core for the 250°F seawater and 150 ppm P-tagged sulfonated polymer experiment.

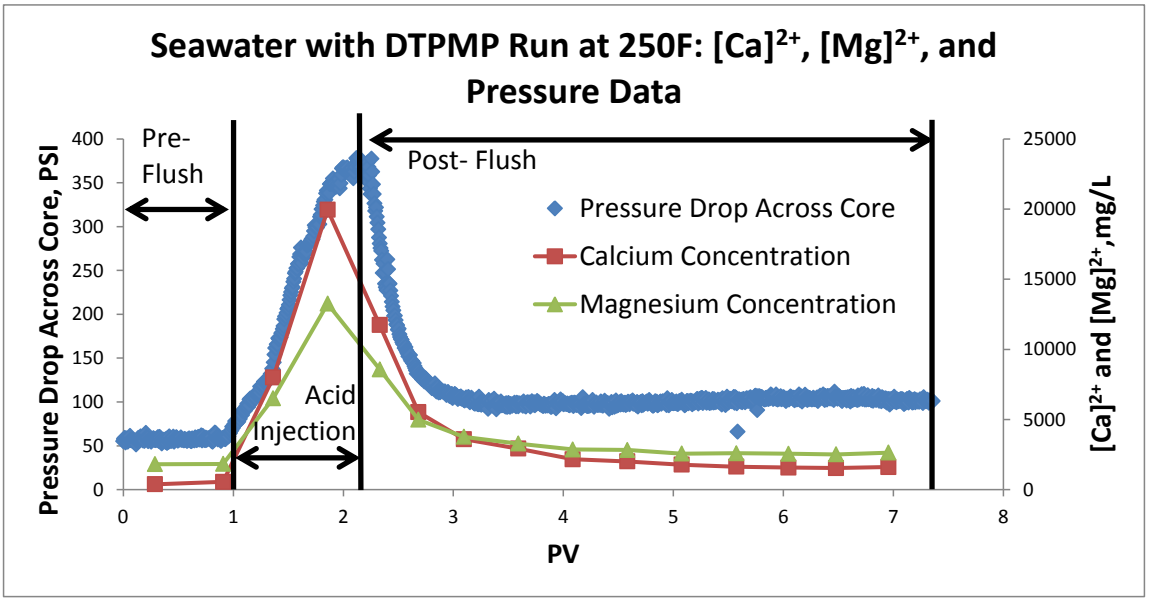

Figure 45: Graph of pressure drop across the tested core compared to dissolved calcium and magnesium concentrations within collected effluent samples for the 250°F seawater and 150 ppm P-tagged sulfonated polymer experiment.

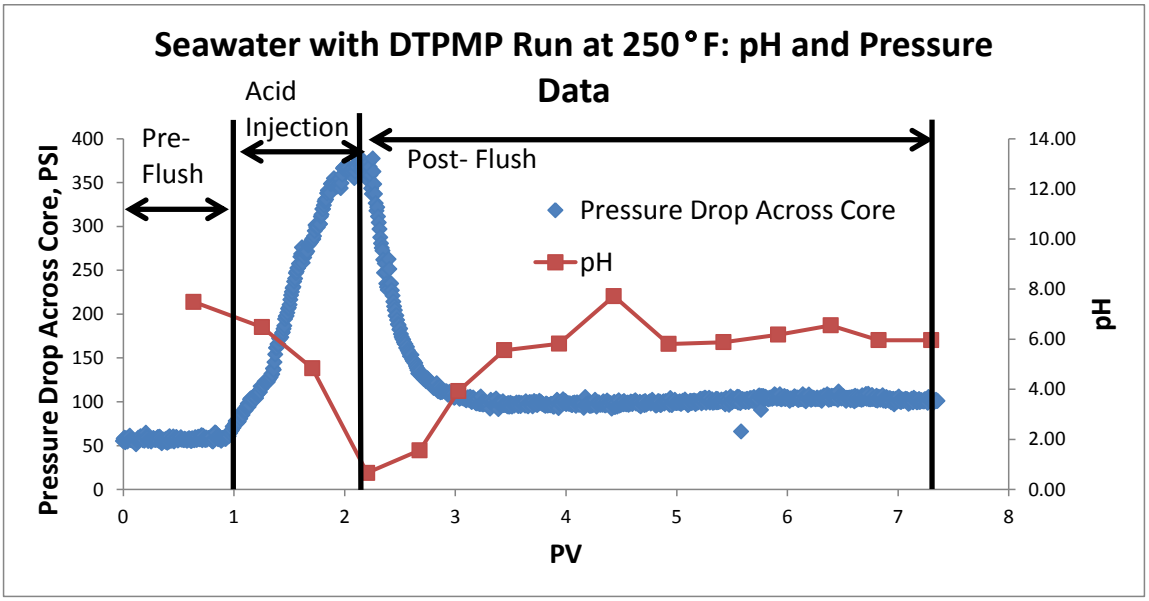

Figure 46: Graph of pressure drop across the tested core compared to the pH of the collected effluent samples for the 250°F seawater and 150 ppm P-tagged sulfonated polymer experiment.

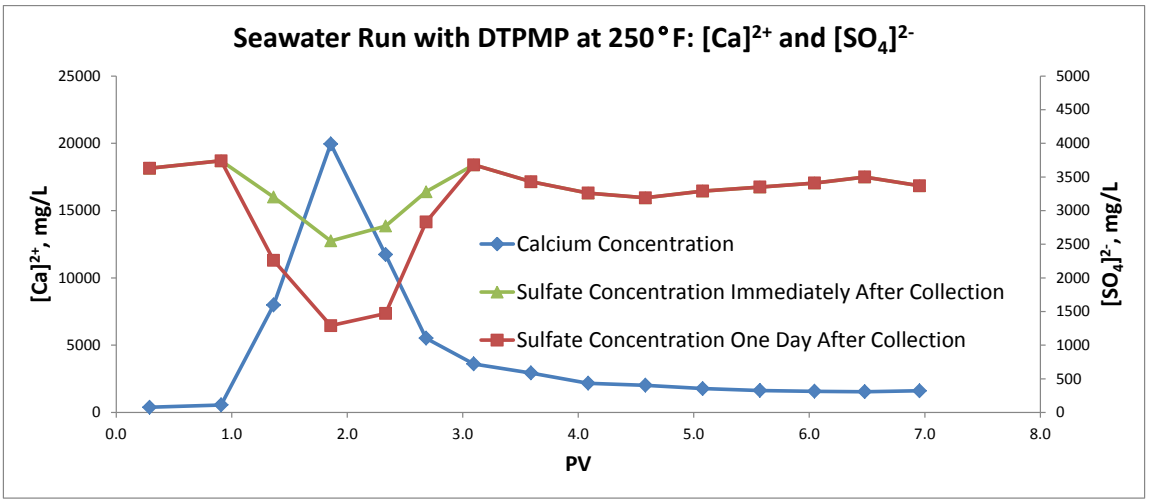

Figure 47: Graph of sulfate concentration in effluent samples measured immediately after collection and one day after collection compared to dissolved calcium concentration within collected effluent samples for the 250°F seawater and 150 ppm P-tagged sulfonated polymer experiment.

Corefloods at 150°F were not run since P-tagged sulfonated polymer scale inhibitor has proven to have limited effectiveness. The limitation is due to large polymer molecules not being able to fit through small pore throats.

4.2.3 Sulfonated Polymer

Sulfonated polymer scale inhibitor was not tested in corefloods due to sulfonated polymer containing long polymer chains that would block pores similar to what occur in the P-tagged sulfonated polymer corefloods.

4.2.4 DTPMP

The test run using DTPMP to inhibit scale formation during the coreflood with seawater at 77°F and HCl to acid stimulate dolomite showed a permeability increase at the end of the test. Samples collected and tested for SO_4^{2-} during the tests showed that less sulfate precipitation occurred while the experiment was running than in the test without scale inhibitors at 77°F. After one day, calcium sulfate precipitated out of solution within the collected samples to bring the total amount of precipitation to an amount comparable to the coreflood with seawater and no scale inhibitors at 77°F. The delayed response indicates that the DTPMP adsorbed onto the surface of the core and was not present within the test tubes. Further, the k_f/k_i ratio for the core used in this coreflood was 22.84, which is much higher than the stimulation found in the DI Water coreflood at 77°F. Figure 48 shows the pressure drop across the core, Figure 49 shows the comparison of pressure drop across the core to calcium and magnesium

concentrations within the collected effluent samples, Figure 50 shows a comparison of pH from the collected effluent samples to pressure drop across the core, and Figure 51 shows a comparison of sulfate concentration in collected effluent samples immediately after collection and one day after collection against calcium concentration within collected effluent samples. All these graphs show that the ending condition of the core was such that no acid breakthrough occurred and no further reactions would occur within the core after the experiment.

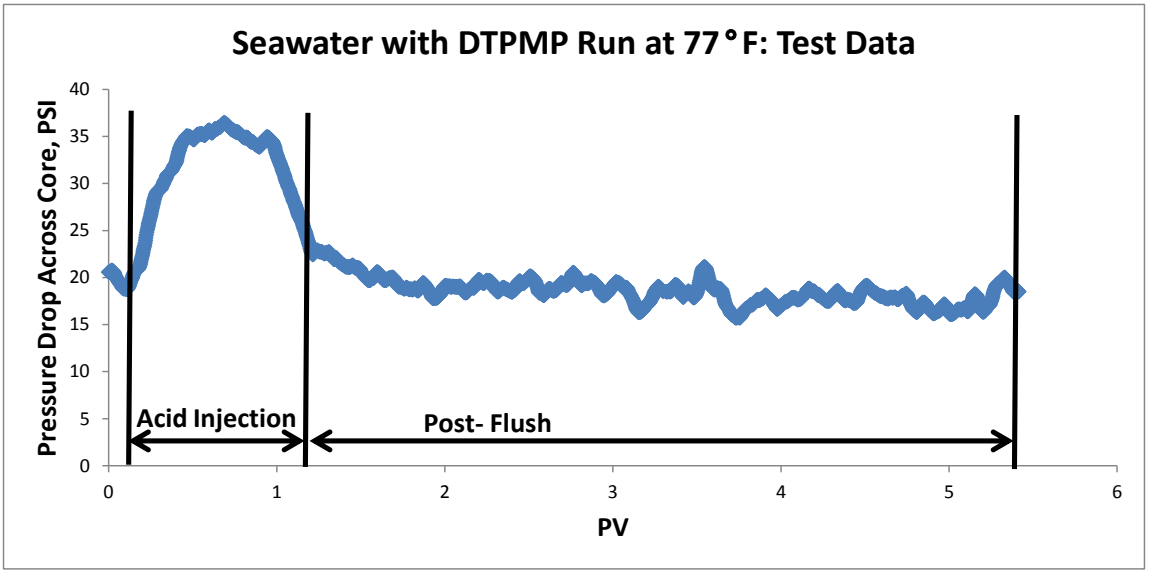

Figure 48: Graph of pressure drop across the tested core for the 77°F seawater and 150 ppm DTPMP experiment.

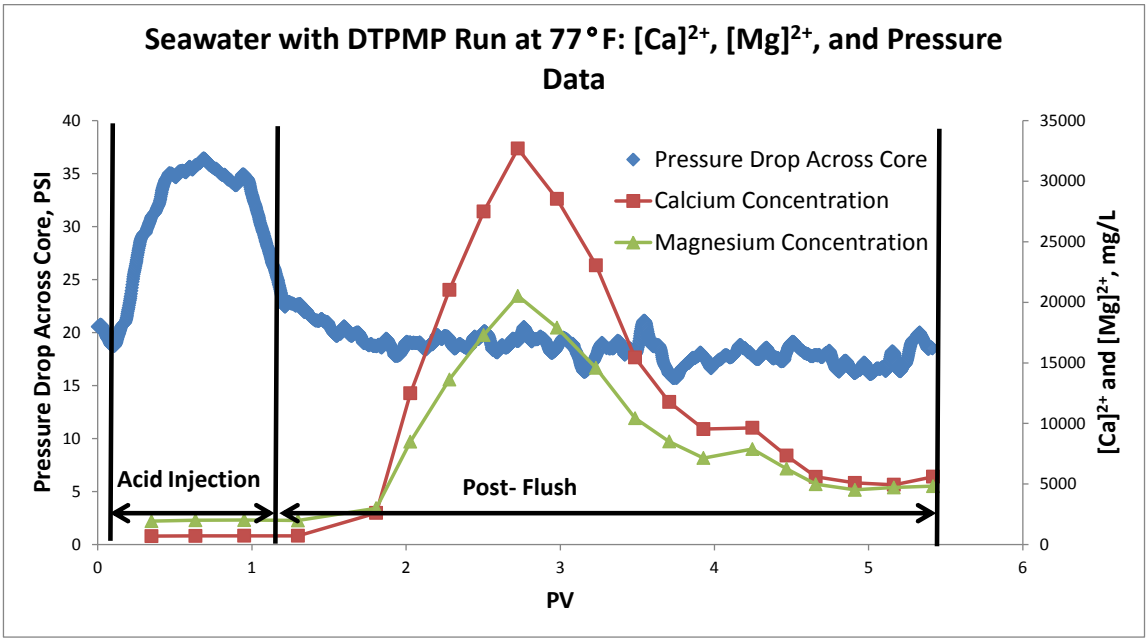

Figure 49: Graph of pressure drop across the tested core compared to dissolved calcium and magnesium concentrations within collected effluent samples for the 77°F seawater and 150 ppm DTPMP experiment.

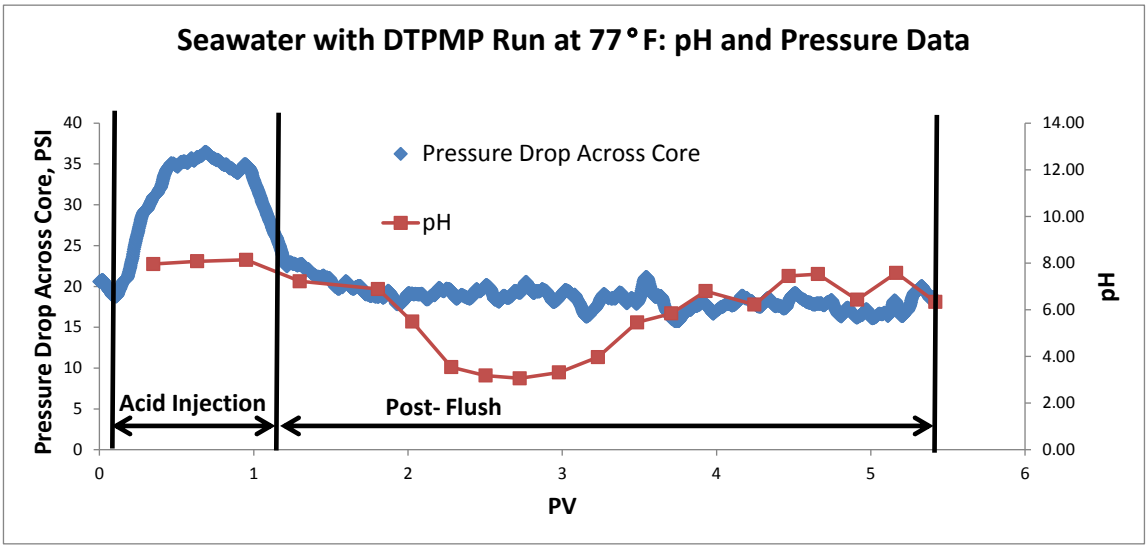

Figure 50: Graph of pressure drop across the tested core compared to the pH of the collected effluent samples for the 77°F seawater and 150 ppm DTPMP experiment.

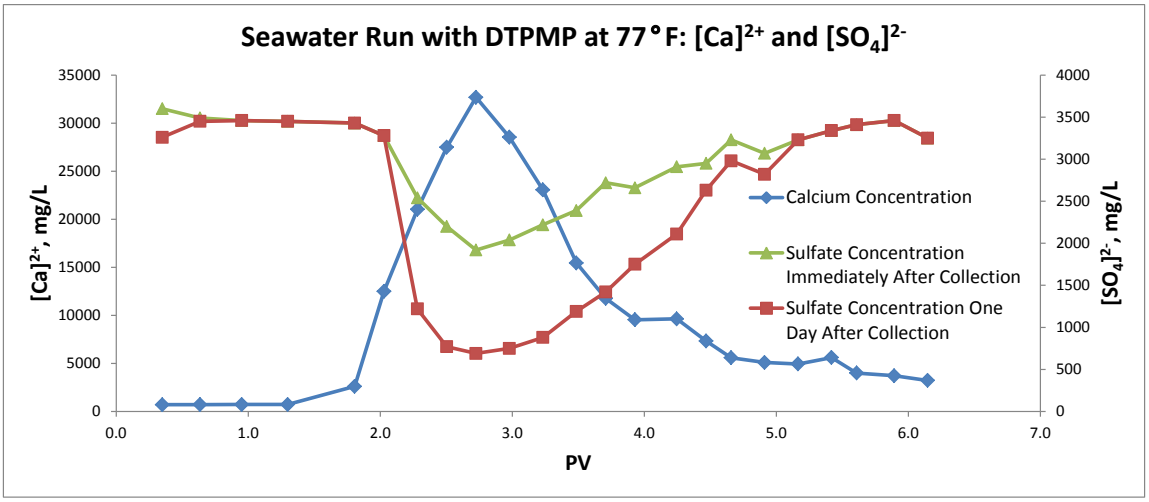

Figure 51: Graph of sulfate concentration in effluent samples measured immediately after collection and one day after collection compared to dissolved calcium concentration within collected effluent samples for the 77°F seawater and 150 ppm DTPMP experiment.

The test run using DTPMP to inhibit scale formation during the coreflood with seawater at 150°F and HCl to acid stimulate dolomite showed a permeability increase at the end of the test in a similar manner to the 77°F test but with greater permeability enhancement. The k_f/k_i ratio for the core used in this coreflood is 40.83, which is much larger than the ratio for the core from the coreflood using DI Water at 150°F. Samples collected and tested for SO_4^{2-} during the tests showed that less sulfate precipitation occurred while the experiment was running compared to the coreflood at 150°F with seawater and no scale inhibitor. After a day, calcium sulfate precipitated out of solution within the collected samples to make the total amount of precipitation equivalent to the total amount of precipitation that occurred in the seawater coreflood with no scale inhibitor at 150°F. The delayed response indicates that DTPMP adsorbed onto the core during the coreflood and was not present in the test tube. Figure 52 shows the pressure

drop across the core, Figure 53 shows the comparison of pressure drop across the core to calcium and magnesium concentrations within the collected effluent samples, Figure 54 shows a comparison of pH from the collected effluent samples to pressure drop across the core, and Figure 55 shows a comparison of sulfate concentration in collected effluent sample immediately after collection and one day after collection against calcium concentration within collected effluent samples. All these graphs show that the ending condition of the core was such that no further reactions would occur within the core after the experiment and no acid breakthrough occurred during the experiment.

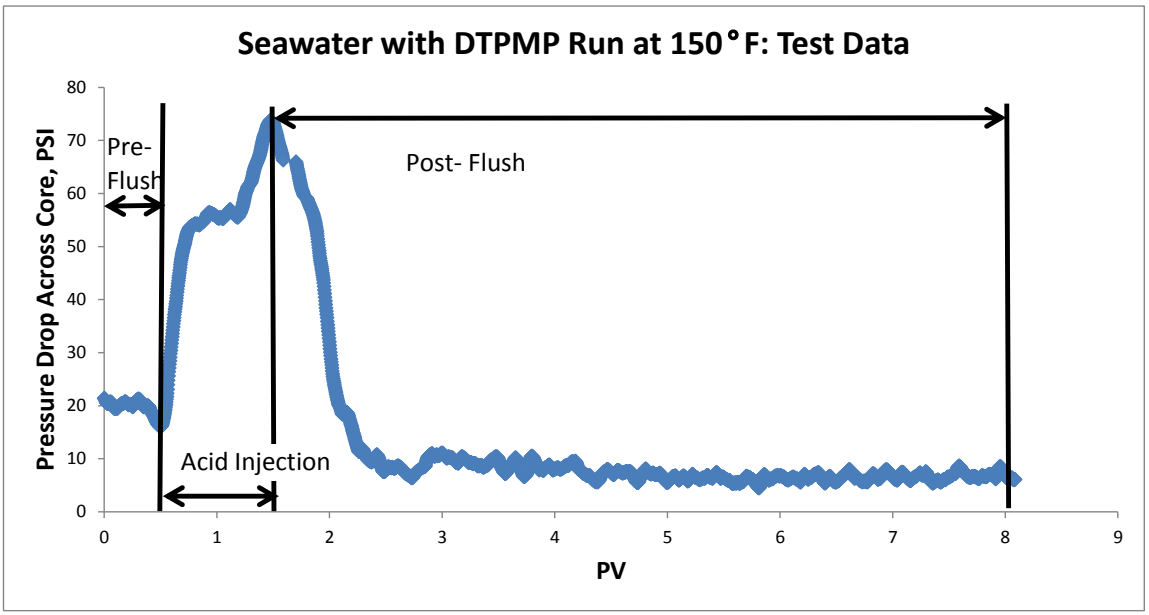

Figure 52: Graph of pressure drop across the tested core for the 150°F seawater and 150 ppm DTPMP experiment.

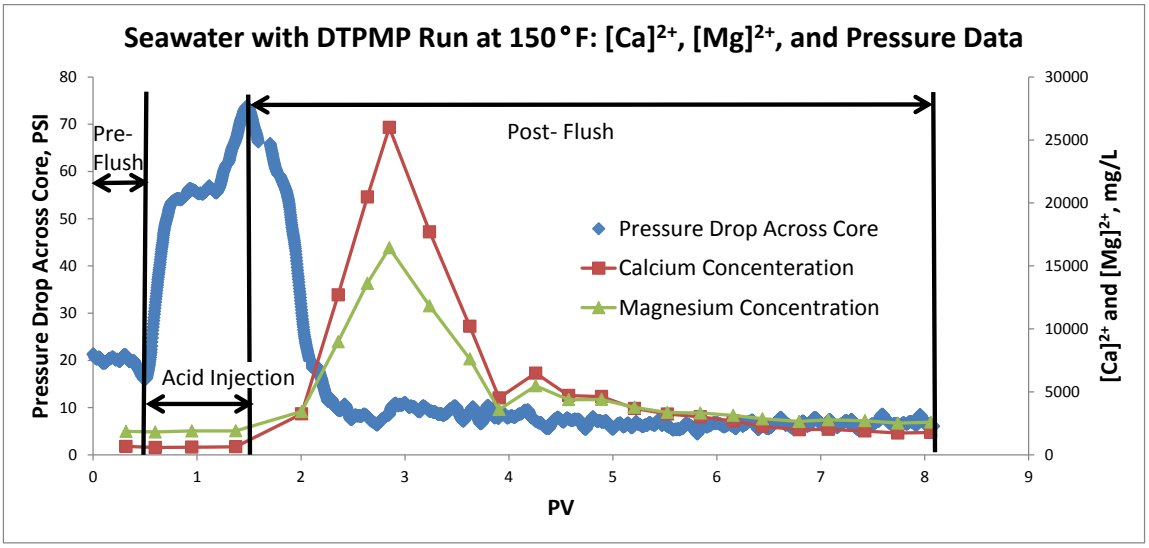

Figure 53: Graph of pressure drop across the tested core compared to dissolved calcium and magnesium concentrations within collected effluent samples for the 150°F seawater and 150 ppm DTPMP experiment.

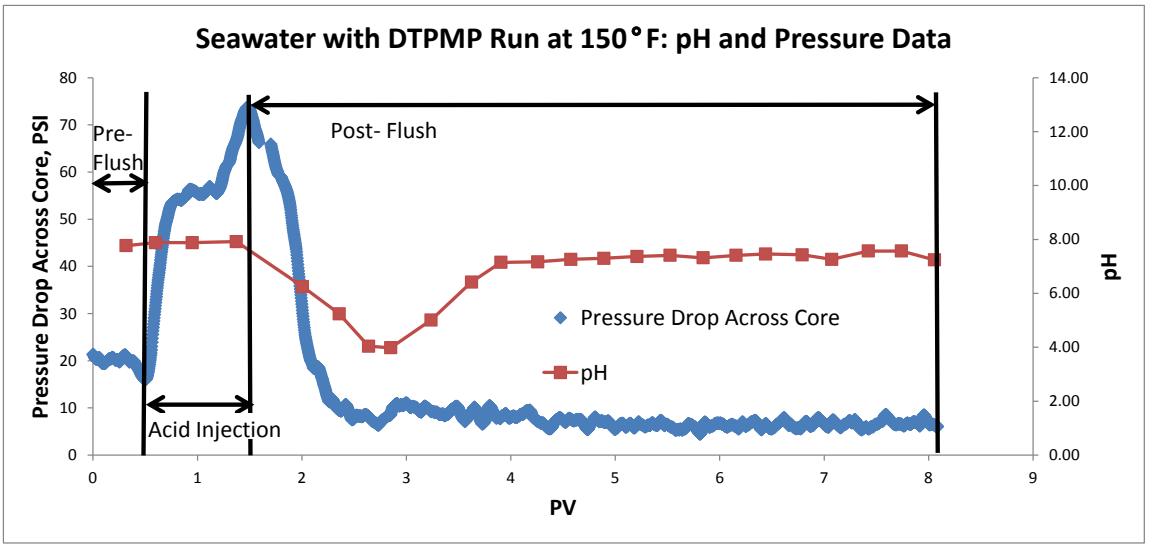

Figure 54: Graph of pressure drop across the tested core compared to the pH of the collected effluent samples for the 150°F seawater and 150 ppm DTPMP experiment.

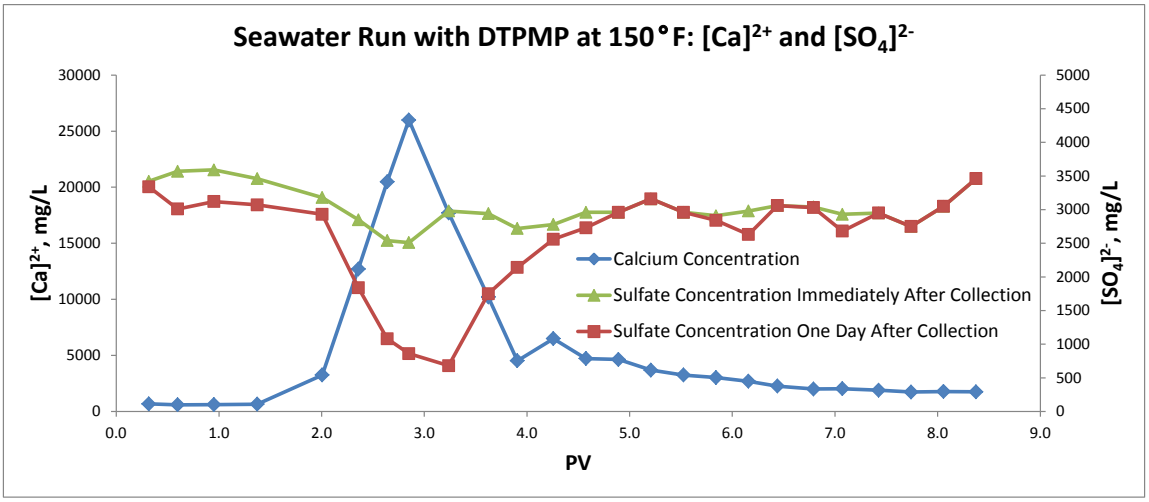

Figure 55: Graph of sulfate concentration in effluent samples measured immediately after collection and one day after collection compared to dissolved calcium concentration within collected effluent samples for the 150°F seawater and 150 ppm DTPMP experiment.

The test run using DTPMP to inhibit scale formation during the coreflood with seawater at 250°F showed a permeability increase at the end of the test, but with a much lower permeability enhancement than the coreflood with seawater and DTPMP at 150°F test. The permeability enhancement for the core in this coreflood was a k_f/k_i ratio of 1.54, which was slightly larger than the amount of stimulation noted in the DI Water coreflood at 250°F. Samples collected and tested for SO_4^{2-} during the tests showed that a moderate amount of sulfate precipitation occurred while the experiment was running. After one day, calcium sulfate precipitated out of solution within the collected samples so that the total amount of sulfate precipitation in samples from this coreflood matched the amount of precipitation in the samples from the coreflood with seawater and no scale inhibitors at 250°F. The larger amount of initial precipitation coupled with the reduced stimulation enhancement show that DTPMP started to thermally degrade at 250°F.

However, DTPMP is still an effective scale inhibitor for these conditions. Figure 56 shows the pressure drop across the core, Figure 57 shows the comparison of pressure drop across the core to calcium and magnesium concentrations within the collected effluent samples, Figure 58 shows a comparison of pH from the collected effluent samples to pressure drop across the core, and Figure 59 shows a comparison of sulfate concentration in collected effluent sample immediately after collection and one day after collection against calcium concentration within collected effluent samples. All of these graphs show that the ending condition of the core was such that no acid breakthrough occurred and no further reactions would occur within the core after the experiment.

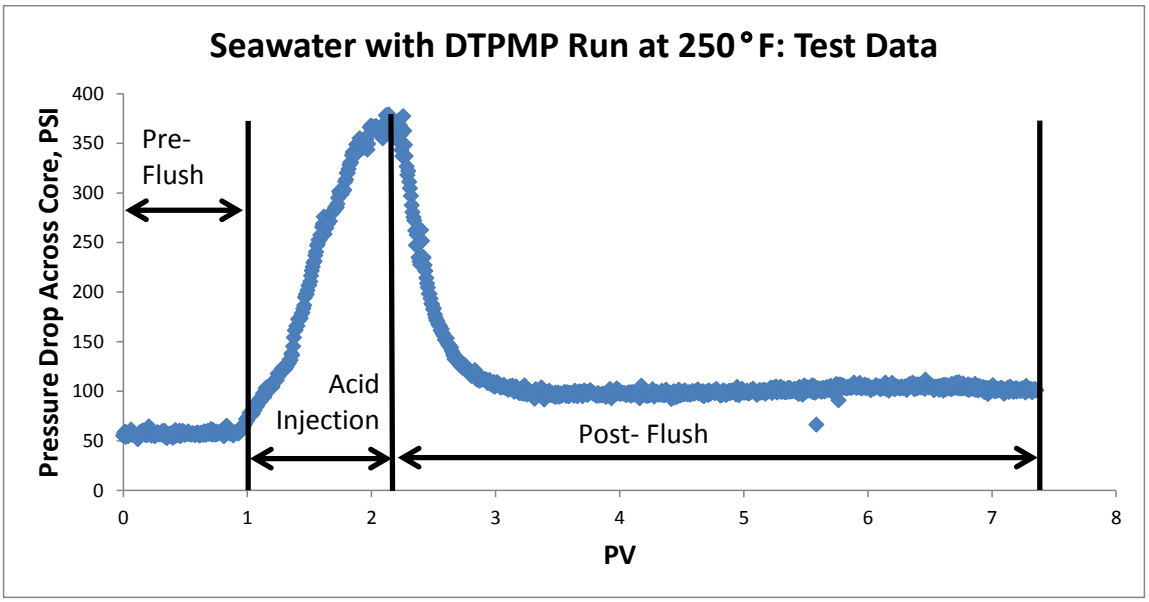

Figure 56: Graph of pressure drop across the tested core for the 250°F seawater and 150 ppm DTPMP experiment.

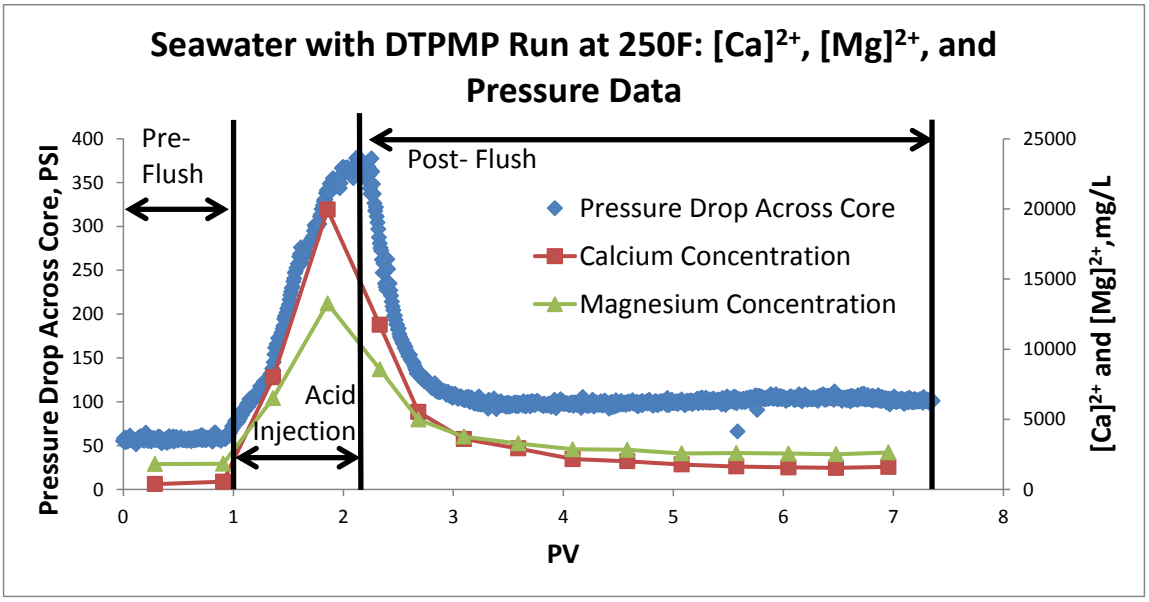

Figure 57: Graph of pressure drop across the tested core compared to dissolved calcium and magnesium concentrations within collected effluent samples for the 250°F seawater and 150 ppm DTPMP experiment.

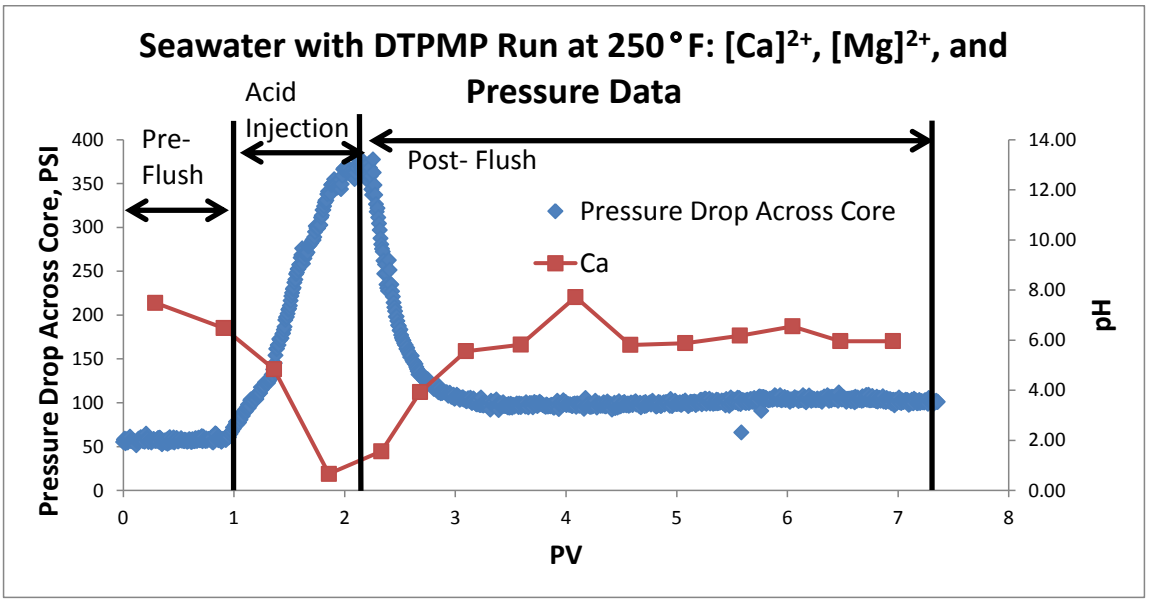

Figure 58: Graph of pressure drop across the tested core compared to the pH of the collected effluent samples for the 250°F seawater and 150 ppm DTPMP experiment.

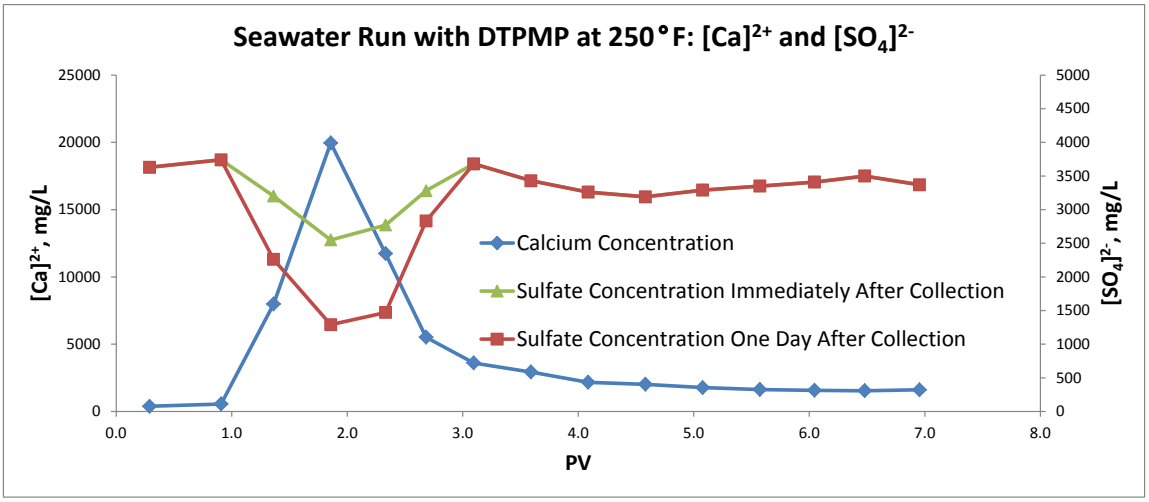

Figure 59: Graph of sulfate concentration in effluent samples measured immediately after collection and one day after collection compared to dissolved calcium concentration within collected effluent samples for the 250°F seawater and 150 ppm DTPMP experiment.

4.3 Discussion

While BHMT, DTPMP, sulfonated polymer, and P-tagged sulfonated polymer were all effective scale inhibitors in the static jar tests, only DTPMP proved to be an effective scale inhibitor in the corefloods. The polymer based scale inhibitors were not effective due to the large polymer chains clogging pores and pore throats within the low permeability dolomite cores tested in these experiments. DTPMP reached its effective thermal limit at 250°F and is not recommended for use at higher temperatures.

Another benefit of using DTPMP as a scale inhibitor is the enhanced stimulation effect compared with DI Water without scale inhibitors. In these tests, with 150 ppm DTPMP added to the stimulating fluid, a stimulation enhancement of 20-30 times the k_f/k_i ratios were obtained within the thermal limits of DTPMP. Table 8 shows a

summary of the initial and final core properties for the cores used within these experiments.

Table 8: Summary of initial and final core conditions for all corefloods (with and without scale inhibitors).

		Porosity (%)	PV (cc)	k-initial (mD)	k-final (mD)	kf/ki	Flow Rate (cc/min)
77° F	**DI Water**	8.5	14.76	0.819	0.935	1.14	77
	Seawater	7.3	12.6	0.42	0.39	0.93	77
	P-Tagged Sulfonated Polymer	13.5	21.9	0.468	0.201	0.43	77
	DTPMP	9.08	15.78	0.47	10.7	22.84	77
150° F	**DI Water**	8.2	14.31	2.339	3.1	1.33	150
	Seawater	10.07	17.5	3.39	2.74	0.81	150
	Seawater	7.6	13.13	0.303	0.28	0.92	150
	BHMT	9.6	16.68	0.406	0.318	0.78	150
	DTPMP	8.18	14.21	0.6	24.5	40.83	150
250° F	**DI Water**	9.3	16.16	0.78	1.02	1.31	250
	Seawater	7.6	13.2	2.18	1.55	0.71	250
	P-Tagged Sulfonated Polymer	13.5	21.9	2.586	2.62	1.01	250
	DTPMP	13.95	24.23	2.88	4.43	1.54	250
325° F	**DI Water**	9.02	15.69	1.18	13	10.89	2
	DI Water	13	21.1	1.204	110	91.36	325
	Seawater	15.8	25.6	1.187	5.07	4.27	325

From Table 9, DTPMP tests can be seen to have low amounts of initial precipitation followed by larger amounts of additional precipitation. This behavior is contrary to the behavior of the samples without the use of scale inhibitor; these samples had higher initial amounts of calcium sulfate precipitation followed by additional precipitation. This behavior indicates that the scale inhibitor adsorbed onto the core walls and was not present in the effluent; which is expected for this type of scale inhibitor. The total amount of precipitation that occurred in all cases was within a close range, indicating that no scale inhibitor prevented precipitation for more than a day (in effluent samples). Extrapolating this observation to the field suggests that any stimulation relying on these scale inhibitors should be limited in duration to less than a day if a squeeze treatment has not already been conducted in a zone large enough to encapsulate all reaction products from the well stimulation.

Table 9: Summary of precipitated sulfate and dissolved calcium and magnesium, determined by chemical analysis of collected samples, for each set of seawater experiments.

	150°F - BHMT	77°F - P Tagged Sulfonated Polymer	250°F - P Tagged Sulfonated Polymer
Total Sulfate Injected, mg	690	302	537
Total Sulfate Ejected, mg	619	218	471
Total Sulfate After One Day, mg	494	178	452
Sulfate Precipitated in Core, mg	72	84	66
Additional Sulfate Precipitation After One Day, mg	125	40	19
Total Sulfate Precipitated, mg	197	125	86
Total Dissolved Calcium, mg	569	514	682
Total Dissolved Magnesium, mg	679	591	780

	77°F - DTPMP	150°F - DTPMP	250°F - DTPMP
Total Sulfate Injected, mg	326	399	609
Total Sulfate Ejected, mg	293	363	557
Total Sulfate After One Day, mg	246	311	513
Sulfate Precipitated in Core, mg	34	37	52
Additional Sulfate Precipitation After One Day, mg	47	52	44
Total Sulfate Precipitated, mg	80	89	96
Total Dissolved Calcium, mg	681	549	705
Total Dissolved Magnesium, mg	911	628	735

5. COMPARISON OF DOLOMITE AND LIMESTONE RESULTS

5.1 Summary of Calcite Results

Experiments conducted on dolomite followed the procedures from similar experiments conducted on calcite by He et al. [5c, 5d, 6b] with the exception of injecting 20 mL of HCl through the dolomite cores whereas 10 mL of HCl was injected through calcite cores by He et al. (2012a, 2012b). Twice as much as was injected through the dolomite cores as compared to the calcite cores because dolomite is much less reactive to HCl than calcite. This lowered reactivity and also permitted slower flow rates to be used at elevated temperatures without face dissolution occurring on the dolomite cores.

He et al. (2012a, 2012b) ran corefloods with temperatures up to 210°F in his experiments and observed that the cores experienced a small stimulation effect or were damaged when no scale inhibitors were present. Dolomite cores in the present set of experiments were all damaged up to 250°F when no scale inhibitors were present. However, at 325°F dolomite experienced stimulation. No comparison conclusions can be drawn without data from similar calcite corefloods at 325°F.

The reduced dissolution rate of dolomite compared to calcite reduced the concentration of dissolved calcium. This reduction in dissolved calcium allowed DTPMP to work within the dolomite during matrix acidizing, unlike in calcite which experienced calcium poisoning of the inhibitor [5c]. In a similar situation BHMT worked as a good scale inhibitor in calcite, but precipitated in the acidized dolomite

environment. BHMT did not work well in the dolomite core used due to the presence of iron in the dolomite core catalyzing the precipitation of calcium phosphate.

5.2 Discussion

Previous authors have conducted studies about inhibitor performance in calcite and assumed similar results would occur within dolomite [5d, 6a, 22]. Comparing their results from studies on calcite to the current set of results from this study on dolomite demonstrates that those assumptions are false and no assumptions should be made about inhibitor interactions within dolomite based on calcite tests. Comparing results from the presented experiments with tests by He et al. shows that there are some similarities in dissolved calcium profile shape and sulfate concentration profile shape between the carbonate behaviors. But the concentrations of the chemicals are different and lead to differing results. It is better to test dolomite and calcite independently since they have very different chemical interactions due to chemical composition.

6 SUMMARY AND CONCLUSIONS

6.1 Summary

Corefloods were conducted to determine the amount of damage caused by acidizing HCl in the presence of seawater. Calcium sulfate precipitation was determined to damage dolomite cores injected with HCl at all temperatures, but only required scale inhibitors for temperatures up to 250°F. At 325°F dolomite stimulated in the presence of seawater had half the stimulation of dolomite stimulated with DI Water. Due to the large stimulation effect present in the stimulation of dolomite at 325°F with seawater, it was decided that the core would be considered stimulated, even though the core could be considered damaged in comparison to the DI Water core.

Static jar tests and additional corefloods were conducted to find scale inhibitors which can mitigate scale calcium sulfate scale formation during dolomite stimulation with HCl in the presence of seawater. Four types of scale inhibitors effectively mitigated calcium sulfate precipitation during static jar tests: BHMT, DTPMP, sulfonated polymer, and P-tagged sulfonated polymer. Coreflood tests of the polymer based scale inhibitors showed that the polymer chains were too big to fit through the pores of cores used in these studies. BHMT proved to be ineffective in corefloods because iron was present within the cores which catalyzed the inhibitor to react with free calcium ions to form calcium phosphonate precipitate. DTPMP proved to be an effective scale inhibitor for calcium sulfate for corefloods tests ranging in temperature from 77°F to 250°F. At 250°F DTPMP started to thermally degrade and was not as

effective as it was at lower temperatures. Cores stimulated with acid and DTPMP in the presence of seawater also showed much greater permeability enhancement than cores stimulated with acid and no seawater present.

6.2 Conclusions

From these studies it was shown that seawater should not be present during matrix acidizing of dolomite for temperatures ranging from 77 to 250°F. At 325°F seawater will reduce stimulation effects but not cause a significant amount of damage to the formation. DTPMP proved to be an effective scale inhibitor for mitigating calcium sulfate formation and enhancing stimulation effects within the dolomite for temperature between 77°F and 250°F. Polymer based scale inhibitors were shown to be ineffective scale inhibitors in low permeability cores. Testing the effectiveness of scale inhibitors during acid injection into limestone is not a good indicator for the performance of the scale inhibitor during acid injection into dolomite. Listed below is the full list of conclusions.

- The reaction product of dolomite stimulated with HCl will form calcium sulfate precipitation in the presence of seawater.
- More precipitation occurs in higher permeability cores.
- BHMT was effective at preventing scale formation in limestone but not dolomite for previous tests.

- DTPMP was effective at preventing scale formation in dolomite but not limestone during corefloods.
    - Not all subclasses of carbonates can be treated with the same treatment and each subclass requires independent studies to determine what will or will not work.
- Additional stimulation can be achieved with the addition of scale inhibitors.

REFERENCES

1. (a) Lund, K.; Fogler, H. S.; McCune, C. C., Acidization—I. The dissolution of dolomite in hydrochloric acid. *Chemical Engineering Science* **1973,** *28* (3), 691-IN1; (b) Lund, K.; Fogler, H. S.; McCune, C. C.; Ault, J. W., Acidization—II. The dissolution of calcite in hydrochloric acid. *Chemical Engineering Science* **1975,** *30* (8), 825-835; (c) Taylor, K. C.; Nasr-El-Din, H. A.; Mehta, S. *Anomalous Acid Reaction Rates in Carbonate Reservoir Rocks*. *SPE* 2006.

2. (a) Furby, E.; Glueckauf, E.; L.A; McDonald, The Solubility of Calcium Sulfate in Sodium Chloride and Sea Salt Solutions. *Desalination* **1967,** *4* (2), 264-276; (b) Kan, A. T.; Tomson, M. B., Scale Prediction for Oil and Gas Production. *SPE J.* **2012,** *17* (2), 362-378.

3. Abu-Khamsin, S. A.; Ahmad, S. J. *Laboratory Study on Precipitation of Calcium Sulphate in Berea Sandstone Cores*; SPE 2005.

4. Sorbie, K. S.; Laing, N., How scale inhibitors work: Mechanisms of selected barium sulphate scale inhibitors across a wide temperature range. *SPE* 2004; pp 447-456.

5. (a) BinMerdhah, A. B., Inhibition of Calcium Sulfate and Strontium Sulfate Scale in Waterflood. *SPE Prod. Oper.* **2010,** *25* (4), 545-552; (b) Essel, A. J.; Carlberg, B. L., Strontium Sulfate Scale Control by Inhibitor Squeeze Treatment in the Fateh Field. *JPT, Journal of Petroleum Technology* **1982,** *34* (6), 1302-1306; (c) He, J.; Arensman, D.; Nasr-El-Din, H. A., Effectiveness of Calcium Sulfate Scale Inhibitors in Spent Hydrochloric Acid/Seawater System. *Journal of Petroleum & Environmental Biotechnology* **2013,** *4*, 159-170; (d) He, J.; Mohamed, I. M.; Nasr-El-Din, H. A. *Mitigation of Calcium Sulfate Scale Formation When Seawater Is Used To Prepare HCl-Based Acids*; *SPE* Lafayette, Louisiana, 2012.

6. (a) Berry, S. L.; Boles, J. L.; Smith, K. L., Cost- effective acid stimulation of carbonates using seawater- based systems without calcium sulfate precipitation. *SPE* 2012; Vol. 1, pp 100-112; (b) He, J.; Mohamed, I. M.; Nasr-El-Din, H. A., Potential Formation Damage Due to Preparing HCl Acids Using Seawater. *Canadian Energy Technology & Innovation SPE* **2012,** *1* (4).

7. (a) Shaw, S. S.; Sorbie, K. S.; Boak, L. S., The Effects of Barium Sulfate Saturation Ratio, Calcium, and Magnesium on the Inhibition Efficiency- Part I: Phosphonate Scale Inhibitors. *SPE Prod. Oper.* **2012,** *27* (3), 306-317; (b) Shaw, S. S.; Sorbie, K. S.; Boak, L. S., The effects of barium sulfate saturation ratio, calcium, and magnesium on the inhibition efficiency- part ii: Polymeric scale inhibitors. *SPE* 2012; Vol. 27, pp 390-403.

8. Mumallah, N. A. *Factors Influencing the Reaction Rate of Hydrochloric Acid and Carbonate Rock*; *SPE* 1991.

9. Glasbergen, G.; Kalia, N.; Talbot, M. S. *The Optimum Injection Rate for Wormhole Propagation: Myth or Reality?*; *SPE* 2009.

10. Janecky, D. R.; Seyfried Jr, W. E., The solubility of magnesium-hydroxide sulfate-hydrate in seawater at elevated temperatures and pressures. *American Journal of Science* **1983,** *283* (8), 831-860.

11. Ramsdell, L. S.; Partridge, E. P., The Crystal Forms of Calcium Sulfate. *Journal Mineralogical Society of America* **1929,** *14* (2), 59-74.

12. Nancollas, G. H.; Eralp, A. E.; Gill, J. S. *Calcium Sulfate Scale Formation: A Kinetic Approach*; *SPE J.* 1975.

13. Veerapen, J. P.; Nicot, B.; Chauveteau, G. A., In- Depth Permeability Damage by Particle Deposition at High Flow Rates. *SPE* 2001; pp 333-342.

14. Sorbie, K. S.; Yuan, M. D.; Chen, P.; Todd, A. C.; Wat, R. M. S., Effect of pH on the adsorption and transport of phosphonate scale inhibitor through porous media. *SPE* 1993; pp 149-166.

15. (a) Jordan, M.; Sorhaug, E.; Marlow, D.; Graham, G., "Red" vs. "green" scale inhibitors for extending squeeze life- a case study from north sea, Norwegian sector. *SPE* 2010; (b) Jordan, M. M.; Sorhaug, E.; Marlow, D., Red vs. Green Scale Inhibitors for Extending Squeeze Life-A Case Study From the North Sea, Norwegian Sector- Part II. *SPE Prod. Oper.* **2012,** *27* (4), 404-413.

16. Weijnen, M. P. C.; Van Rosmalen, G. M., Adsorption of phosphonates on gypsum crystals. *Journal of Crystal Growth* **1986,** *79* (1-3), 157-168.

17. Fan, C.; Kan, A. T.; Zhang, P.; Tomson, M. B. *Barite Nucleation and Inhibition at 0 to 200*C With and Without Thermodynamic Hydrate Inhibitors*; *SPE* 2009.

18. Tomson, M. B.; Kan, A. T.; Fu, G.; Shen, D.; Nasr-El-Din, H. A.; Al-Saiari, H.; Al-Thubaiti, M., Mechanistic understanding of rock/ phosphonate interactions and the effect of metal ions on inhibitor retention. *SPE J.* **2008,** *13* (3), 325-336.

19. Inches, C. E.; Sorbie, K. S.; El Doueiri, K., Green inhibitors: Mechanisms in the control of barium sulfate scale. *SPE* 2006.

20. Weijnen, M. P. C.; van Rosmalen, G. M., The influence of various polyelectrolytes on the precipitation of gypsum. *Desalination* **1985,** *54*, 239-261.

21. Kan, A. T.; Fu, G. M.; Tomson, M. B.; Al-Thubaiti, M.; Xiao, A. J., Factors affecting scale inhibitor retention in carbonate- rich formation during squeeze treatment. *SPE J.* **2004,** *9* (3), 280-289.

22. Jordan, M. M. *Simultaneous Well Stimulation and Scale Squeeze Treatments in Carbonate Reservoirs*; *SPE* 2013.